



Metabolic modelling in liver: glucose & galactose

Matthias König

Why liver?

metabolism

Central organ of metabolism

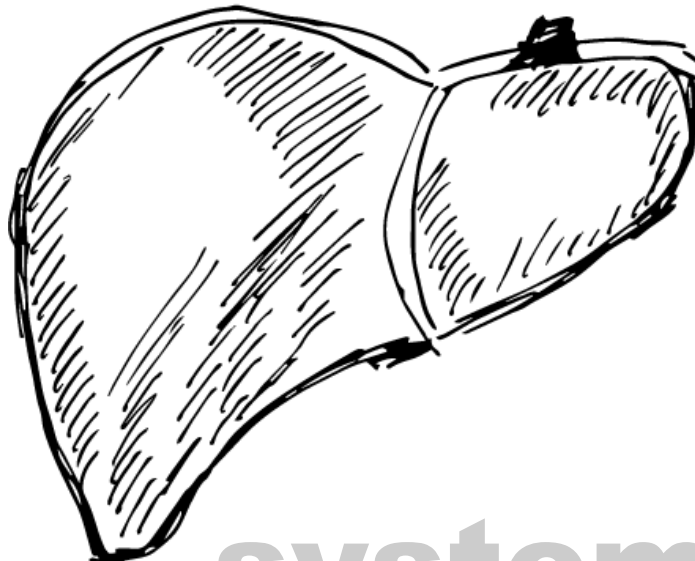
- Metabolic homeostasis
(glucose, amino acids, ...)
- detoxification & clearance

disease

~5 million affected by liver disease in Germany

- Fatty liver (NAFLD/NASH), cirrhosis, hepatitis, alcoholic damage, cancer, ...
- Central role in metabolic diseases like diabetes & metabolic syndrom, NAFDL
- Enormous cost for the health system

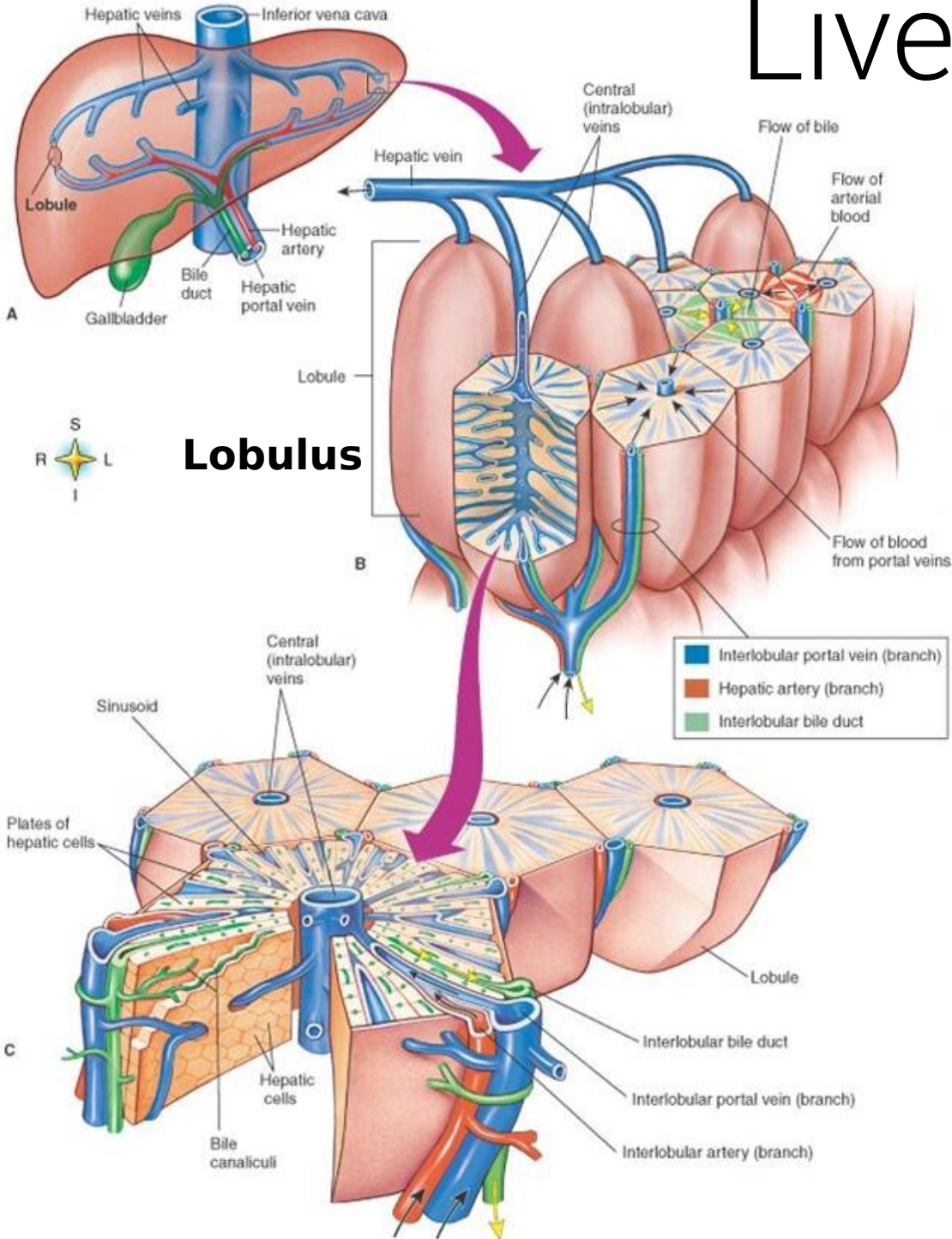
Causes of diseases often remain unknown, despite enormous progress in treatment



system

Liver function is complex interplay of physiology, morphology, perfusion & metabolism on multiple scales

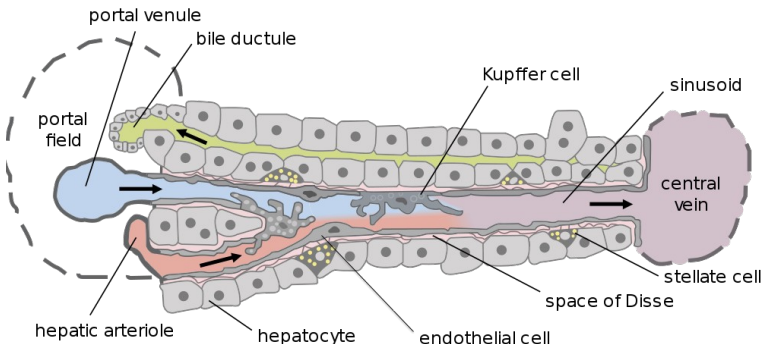
Liver



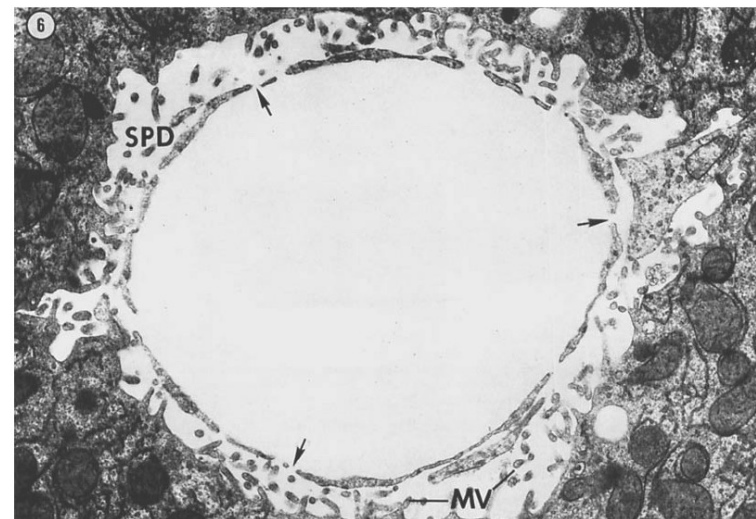
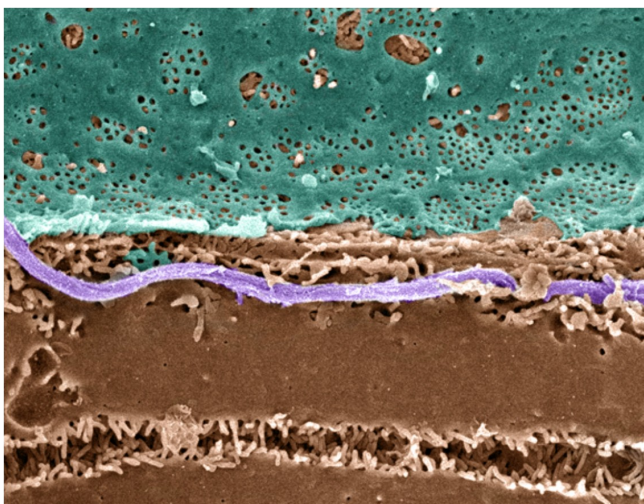
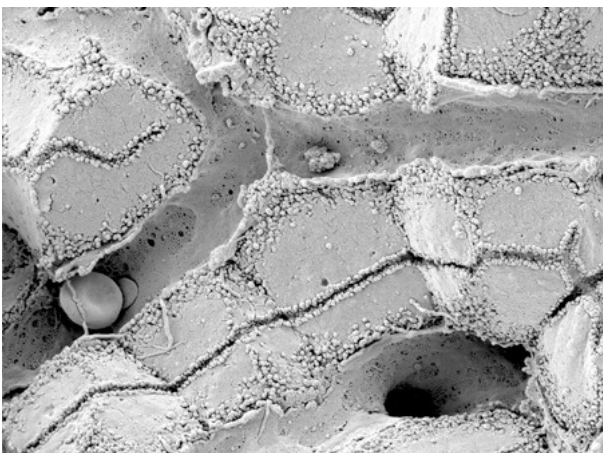
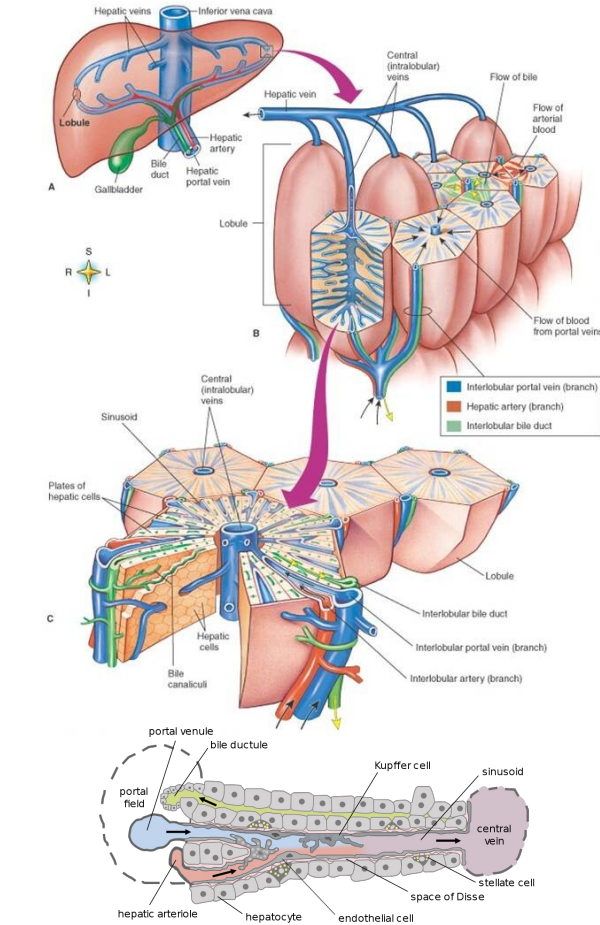
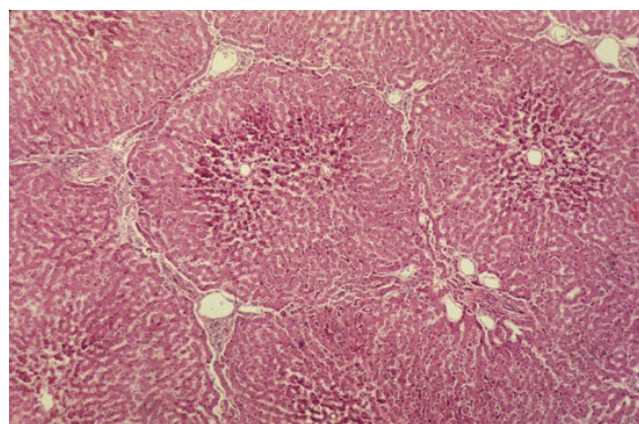
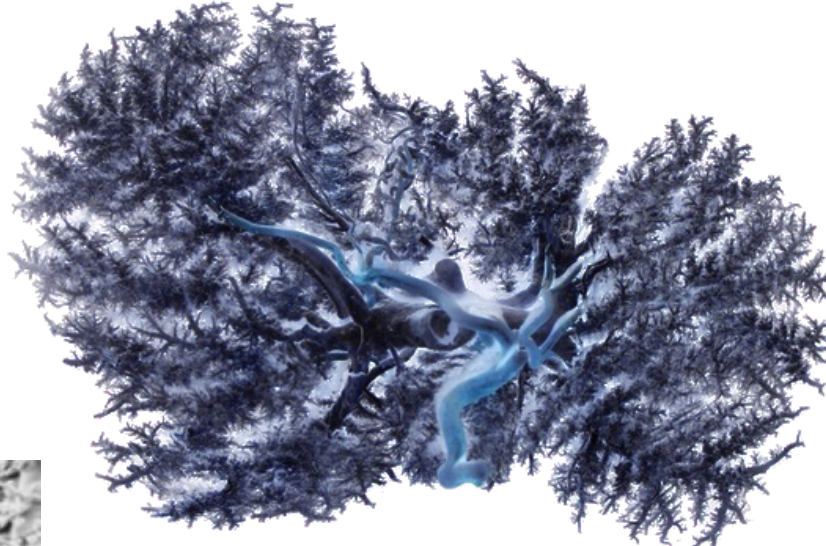
Liver in a nutshell

- Hierarchical architecture
 - Parallel circuit of hexagonal subunits (**lobulus**)
 - Lobulus consists of **network of sinusoids**
 - Hepatocytes main cell type
- Dual blood supply
 - Portal vein (80%)
 - Hepatic artery (20%)

Sinusoidal unit



Hepatocyt



Glucose metabolism

König M. and Holzhütter HG.

Kinetic Modeling of Human Hepatic Glucose Metabolism in T2DM Predicts Higher Risk of Hypoglycemic Events in Rigorous Insulin Therapy

J Biol Chem. 2012

König M., Bulik S. and Holzhütter HG.

Quantifying the Contribution of the Liver to the Homeostasis of Plasma Glucose: A Detailed Kinetic Model of Hepatic Glucose Metabolism Integrated with the Hormonal Control by Insulin, Glucagon and Epinephrine

PLoS Comput Biol. 2012 Jun;8(6):e1002577. Epub 2012 Jun 21.

König M. and Holzhütter HG.

Homeostasis of blood glucose – Computer simulations of central liver functions
systembiologie.de 2014; 8:p.53-57

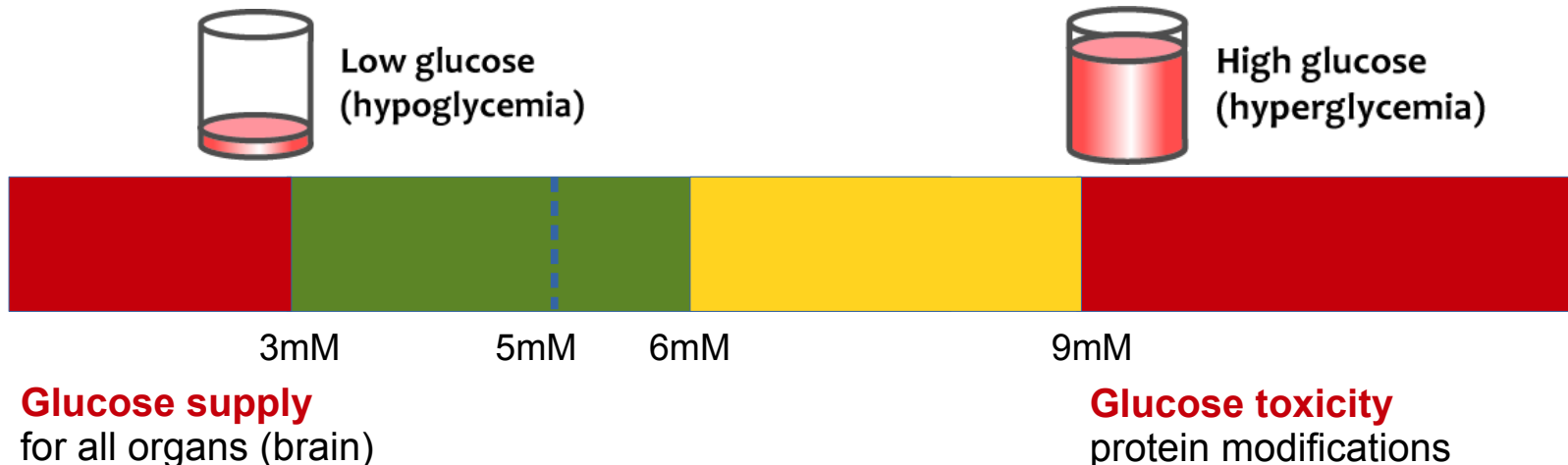
Ricken T. Werner D., Holzhütter HG., König M., Dahmen U., Dirsch O.

Modeling function-perfusion behavior in liver lobules including tissue, blood, glucose, lactate and glycogen by use of a coupled two-scale PDE-ODE approach.

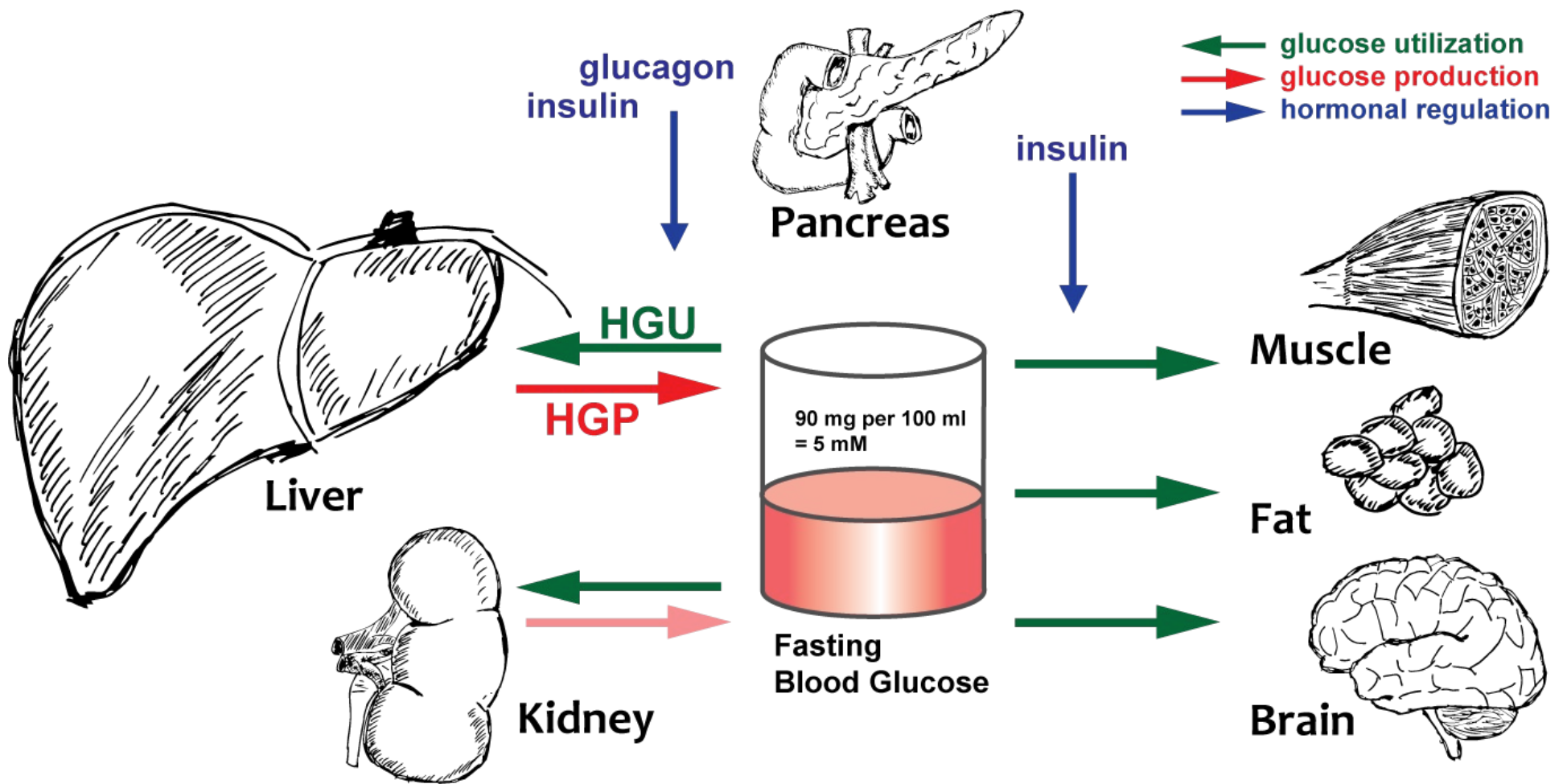
Biomech Model Mechanobiol. 2014 Sep 19.

Glucose level tightly controlled

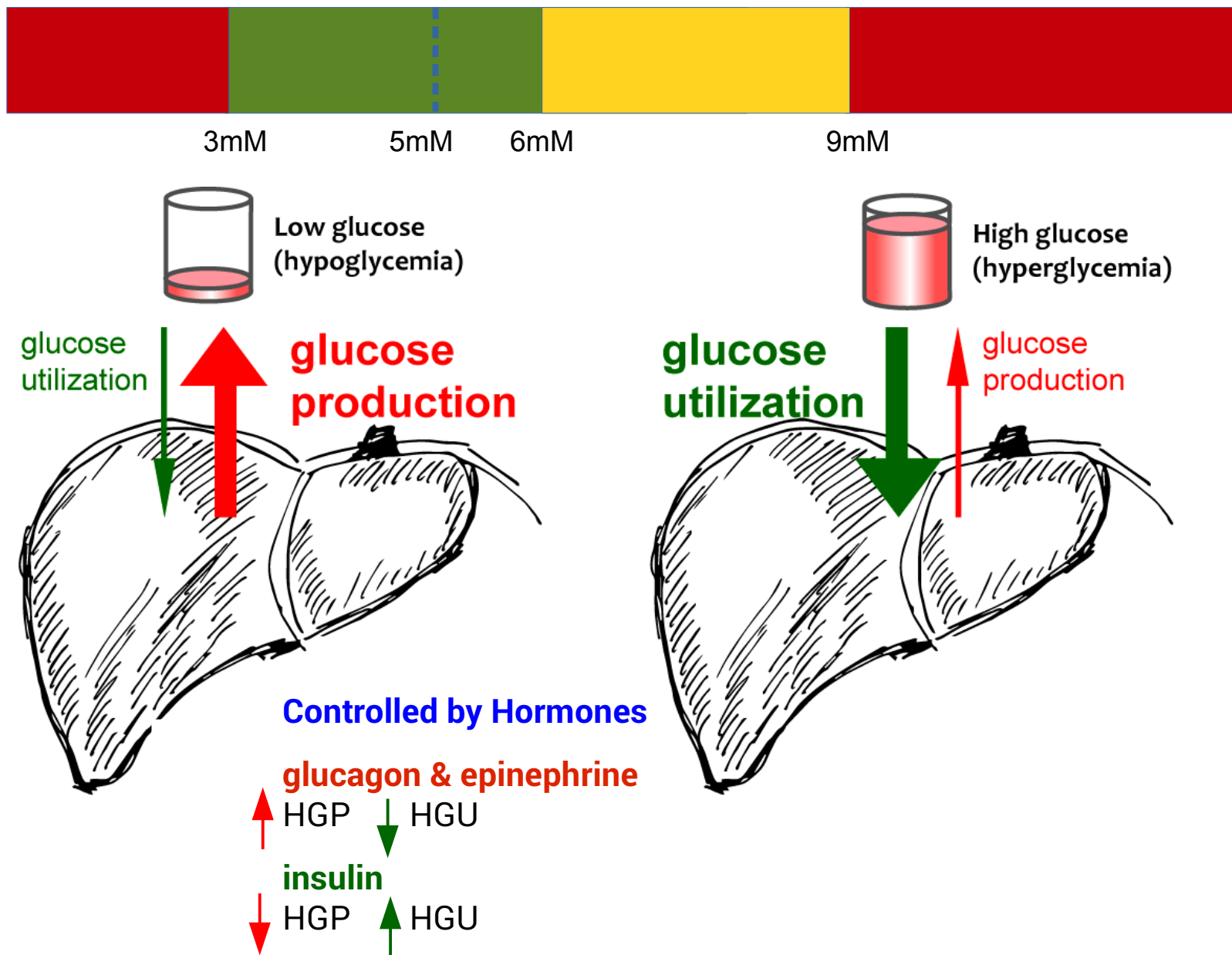
- Plasma glucose almost constant despite large changes in
 - glucose supply (meals)
 - glucose usage (muscle activity)
- $\sim 5\text{mM}$ ($= 80\text{mg/dl}$)
 - min $> 3\text{mM}$: prolonged fasting, intensive muscle activity
 - max $< 9\text{mM}$: postprandial



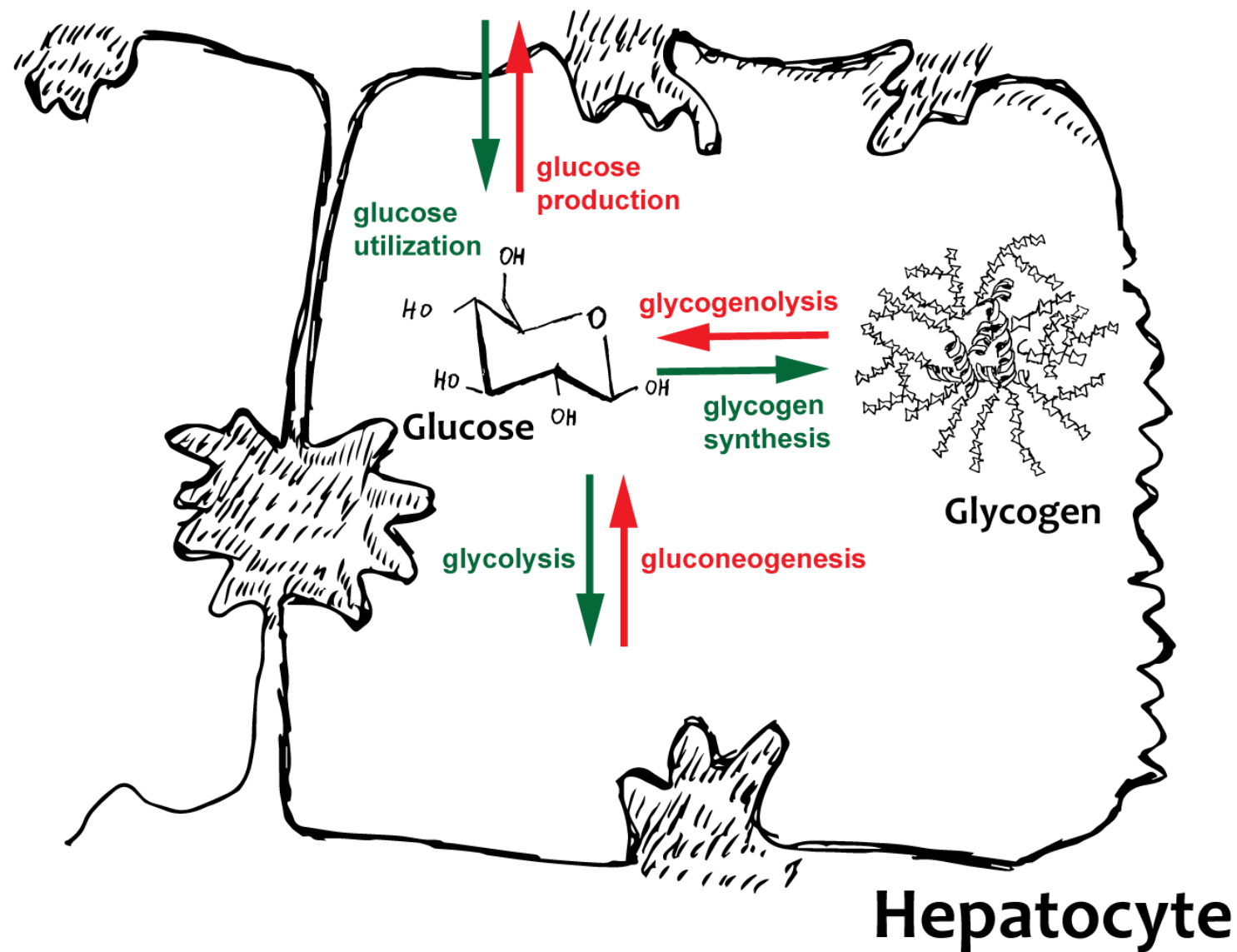
Whole body effects



Dual liver role

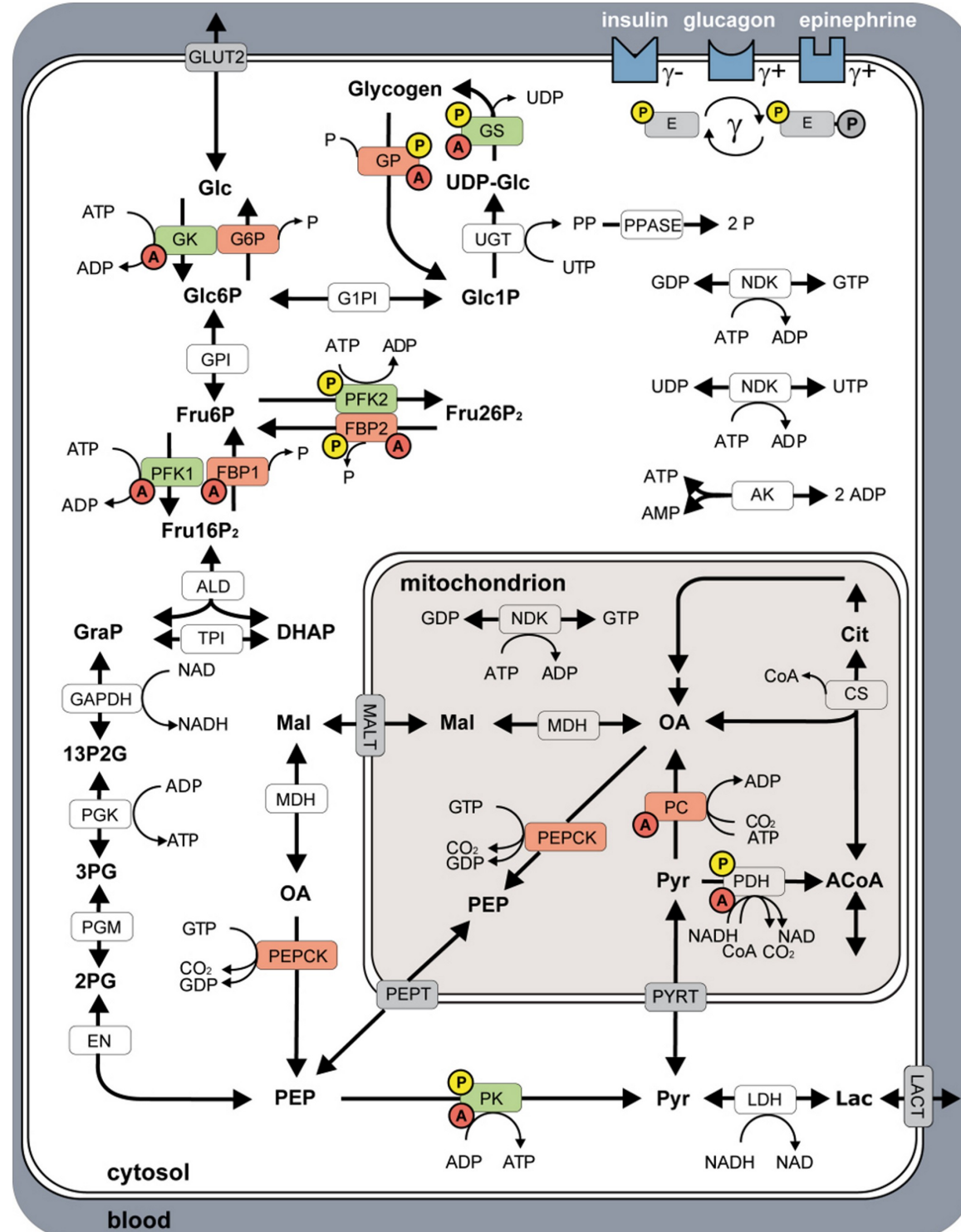


Hepatic glucose metabolism in a nutshell

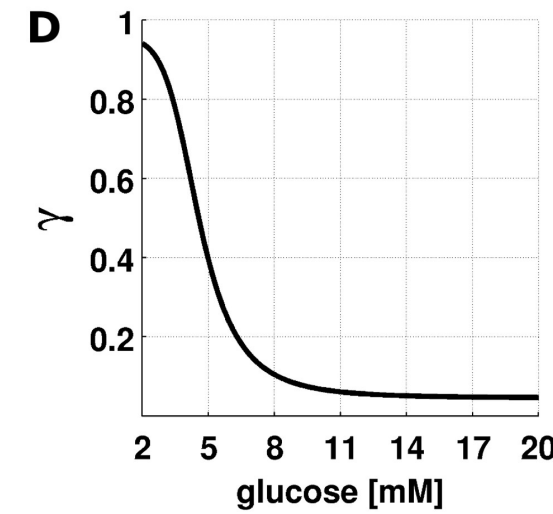
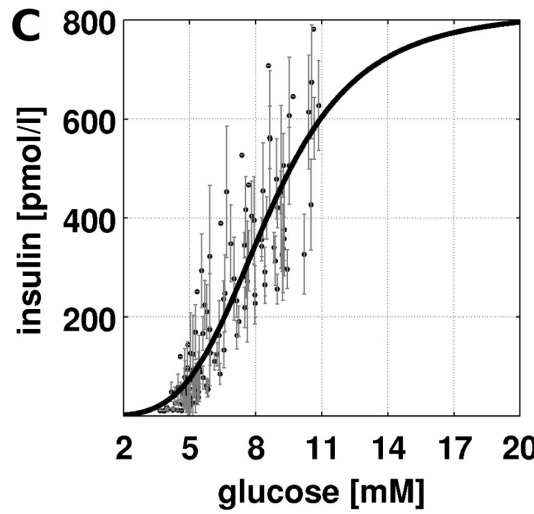
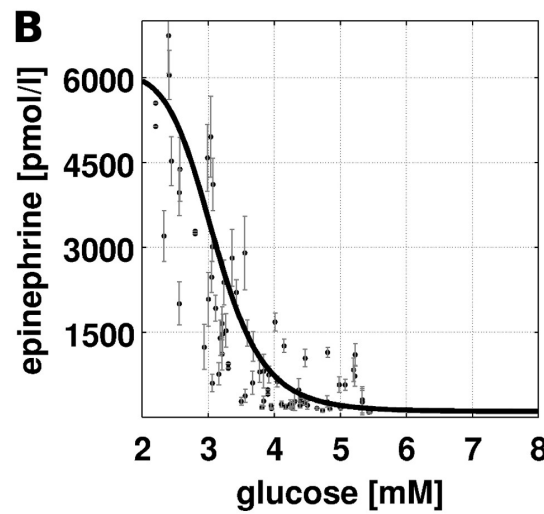
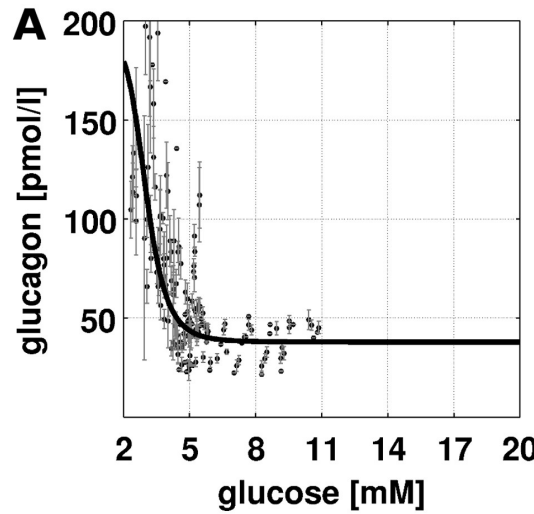


Kinetic Model

- Glycolysis, gluconeogenesis & glycogen metabolism
- Detailed ODE model of human glucose metabolism
 - kinetics for all reactions and transporters
 - hormonal regulation
 - allosteric regulation



Hormonal regulation



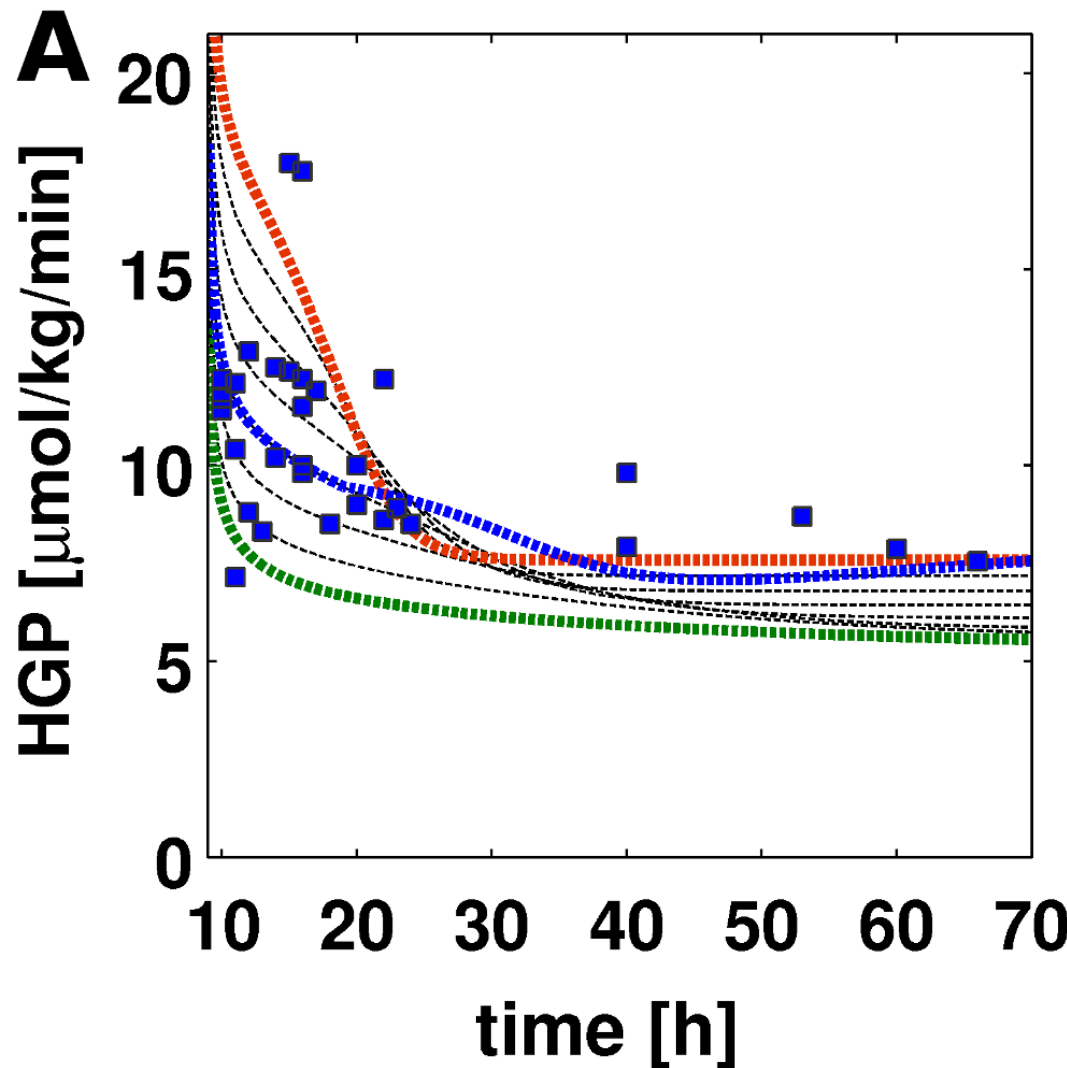
- **Insulin, glucagon and epinephrine** main hormones of glucose homeostasis
- change with blood glucose in a dose response manner
- hormones activate signal cascades which **change phosphorylation state γ of key interconvertible enzymes** of glucose metabolism
- enzyme kinetics depend on phosphorylation state
- depending on glucose level **metabolism is shifted** in direction of **HGP** or **HGU**

Quantifying HGP Contributions

Method	Reference	Time [h]	HGP [$\mu\text{mol/kg/min}$]	GNG [$\mu\text{mol/kg/min}$]	GLY [$\mu\text{mol/kg/min}$]	GNG/HGP [%]
14C-acetate	[Consoli1987]	66	7.56	7.39	0.34	97
13C-NMR	[Rothman1991]	42 – 64	8.7	8.3	0.3	96
13C-glycerol MIDA	[Hellerstein1997]	60	7.87	7.71	1.58	98
13C-glucose MID	[Katz1998]	40	9.8	9.1	1.1	92
2H2O	[Chandramouli1997]	42	NaN	NaN	NaN	93
2H2O	[Staehr2007]	40	7.93	7.13	0.8	90
14C-acetate	[Consoli1987]	14	12.5	3.6	9	28
14C-bicarbonate	[McMahon1989]	10 – 12	7.15	2.2	4.9	31
14C-bicarbonate	[Woerle2006]	12 – 14	8.3	2.6	5.5	31
14C-glucose	[Woerle2003]	12	8.8	4.5	4.3	51
13C-NMR	[Rothman1991]	22	12.2	7.9	4.3	64
13C-NMR	[Magnusson1992]	23	8.9	6.1	2.8	70
13C-glycerol MIDA	[Hellerstein1997]	11	12.1	5.9	6.2	49
13C-glycerol	[Ackermans2001]	10	11.7	4.9	6.8	41
13C-glucose MID	[Katz1998]	12	12.9	5.3	7.7	41
13C-glucose	[Tounian1994]	NaN	13.1	7.4	5.7	56
13C-glucose (a)	[Balasubramanya1999]	18	8.5	5.9	2.6	59
13C-glucose (b)	[Balasubramanya1999]	18	8.5	3.7	4.8	44
13C-glucose	[Ghanaat2005]	12	12.9	5.3	7.6	41
13C-glucose	[Ghanaat2005]	16	11.5	6.6	4.8	57
13C-glucose	[Ghanaat2005]	20	10	7.1	2.9	71
2H2O	[Chandramouli1997]	14	10.2	5.5	4.7	54
2H2O	[Chandramouli1997]	22	8.6	5.5	3.1	64
2H2O	[Chen1999]	16	10	5.5	4.5	55
2H2O	[Chen1999]	20	9	5.4	3.6	60
2H2O	[Chen1999]	24	8.5	5.2	3.3	61
2H2O	[Bisschop2000]	10	11.4	5.5	5.9	48

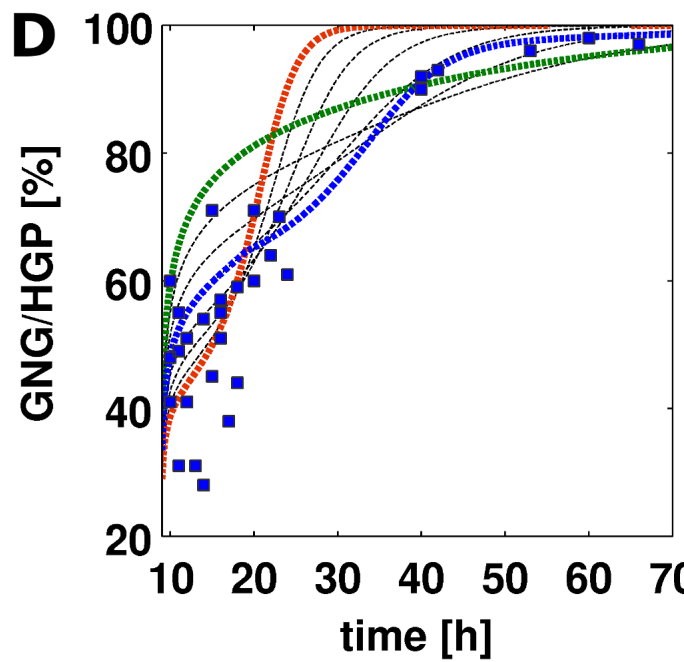
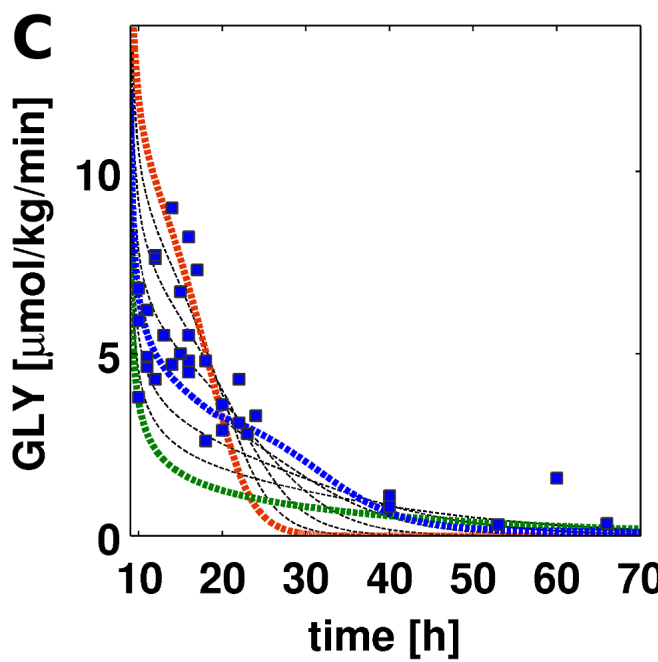
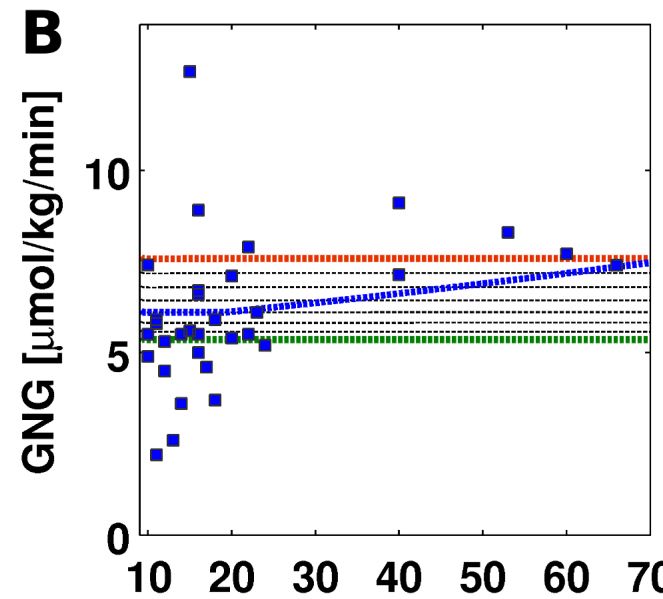
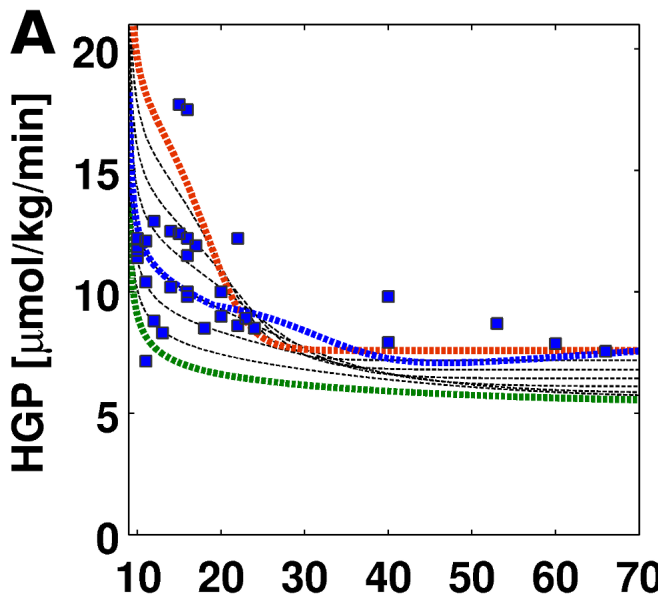
- tracer methods to measure **HGP** and contributions by gluconeogenesis (**GNG**) and glycogenolysis (**GLY**)
- multitude of different studies with different methods

HGP in Short Term Fasting



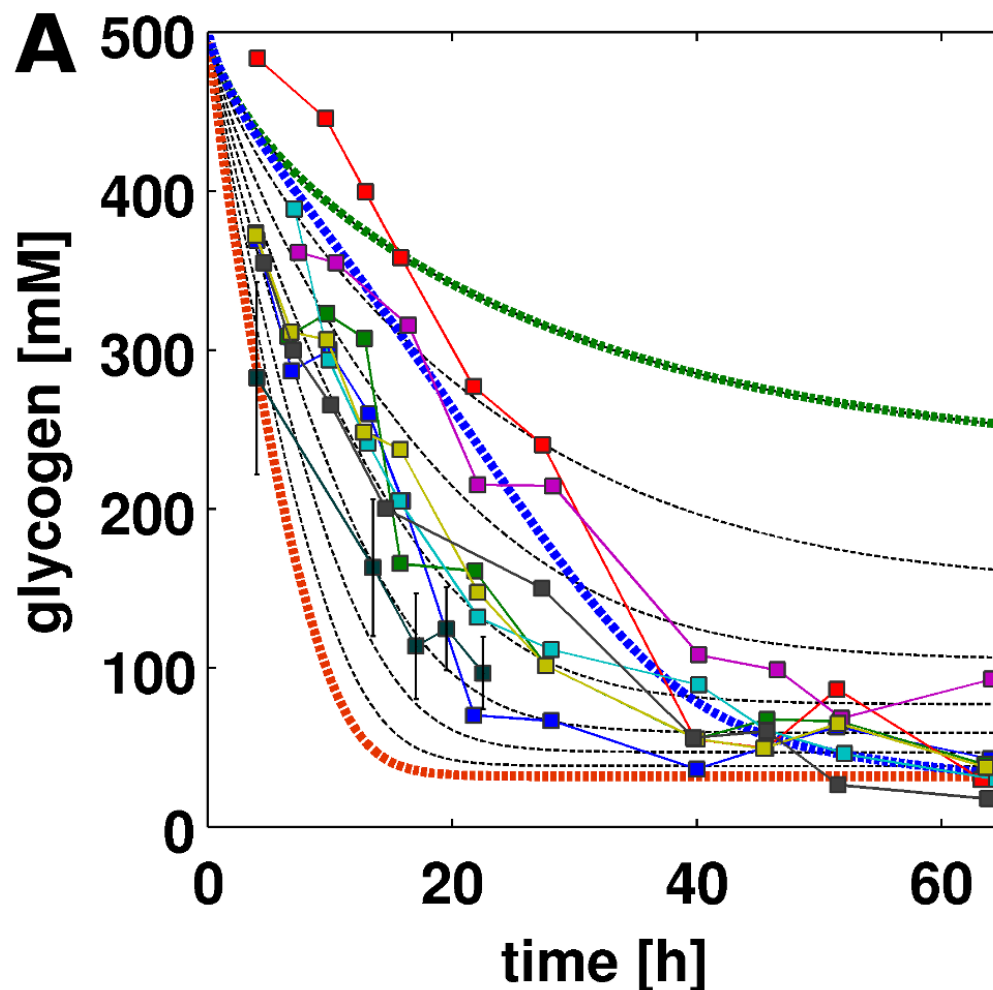
- HGP decreases over time to basal rates of ~7-8 $\mu\text{mol}/\text{min}/\text{kg}$ in ~30h fasting
- Decrease depends on glucose concentration between **5mM** and **3.6mM**
- Taking decreasing plasma glucose into account (**blue**)

Contributions to HGP in Fasting



- Hepatic glucose production (**HGP**) is combination of gluconeogenesis (**GNG**) and glycogenolysis (**GLY**)
- glucose- and time-depending changes in contributions
- very good agreement with exp. data

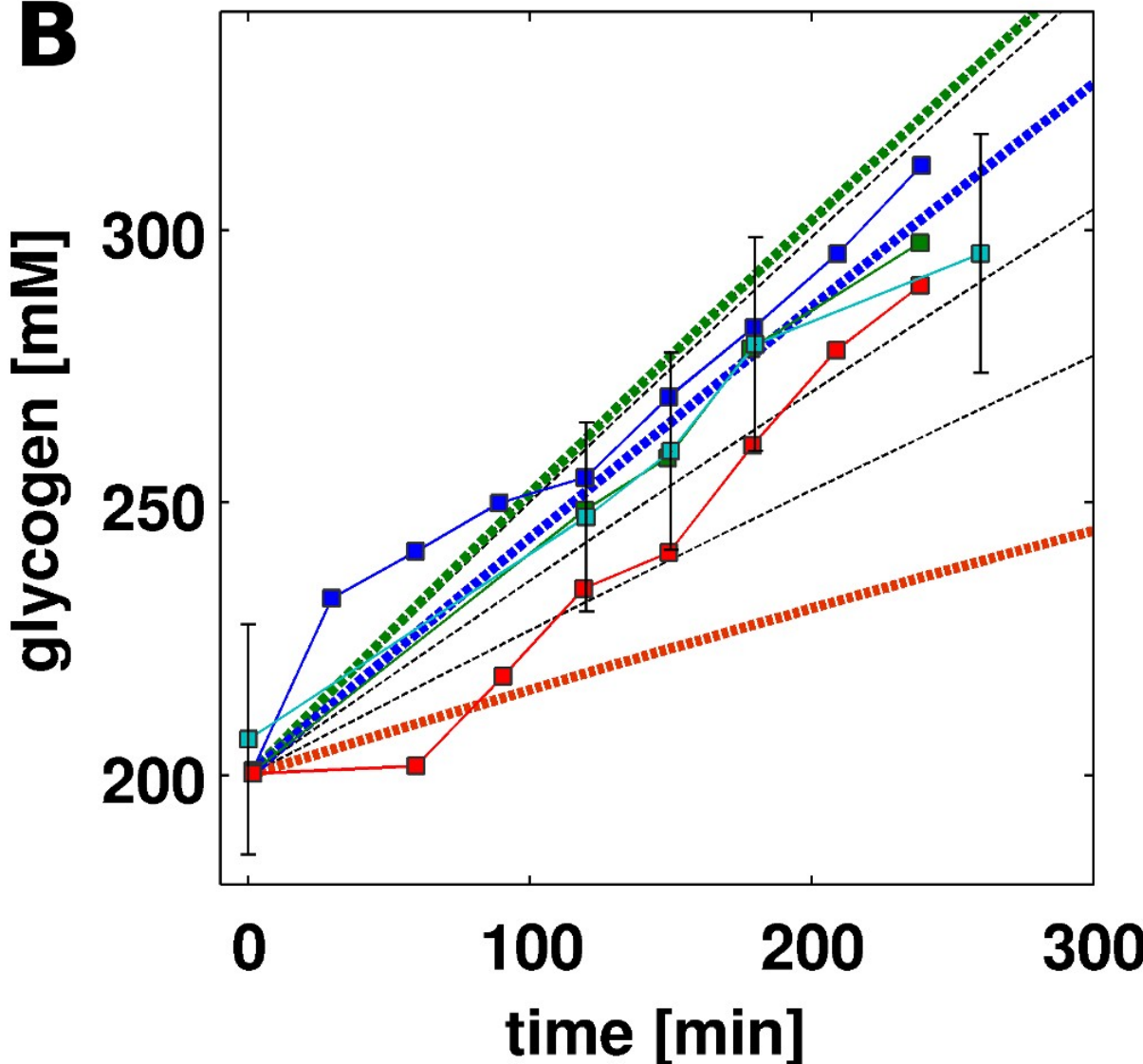
Hepatic Glycogen Decrease



- decrease in glycogen in fasting
 - depending on glucose concentration between **5mM** and **3.6mM**, or taking the decrease in plasma glucose into account (**blue**)
 - very good agreement with experimental data (13C-NMR [Magnusson1992, Rothman1991])

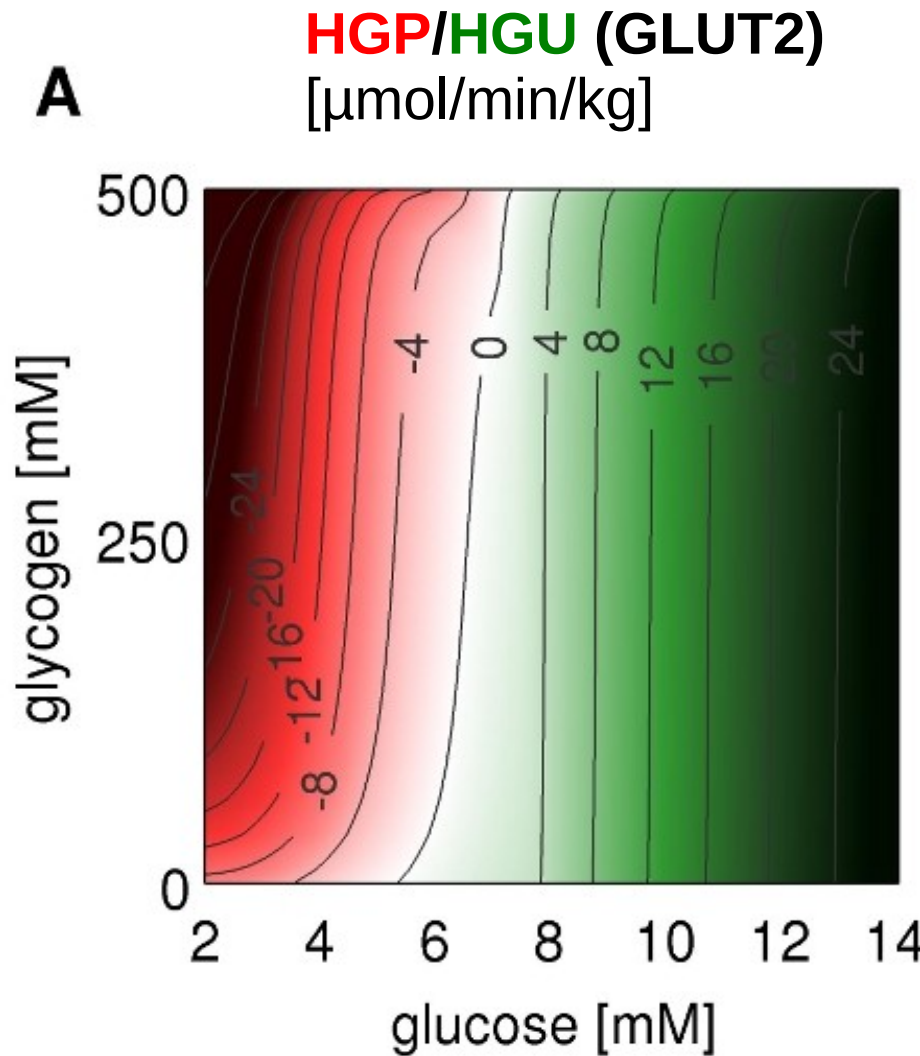
Hepatic Glycogen Synthesis

B



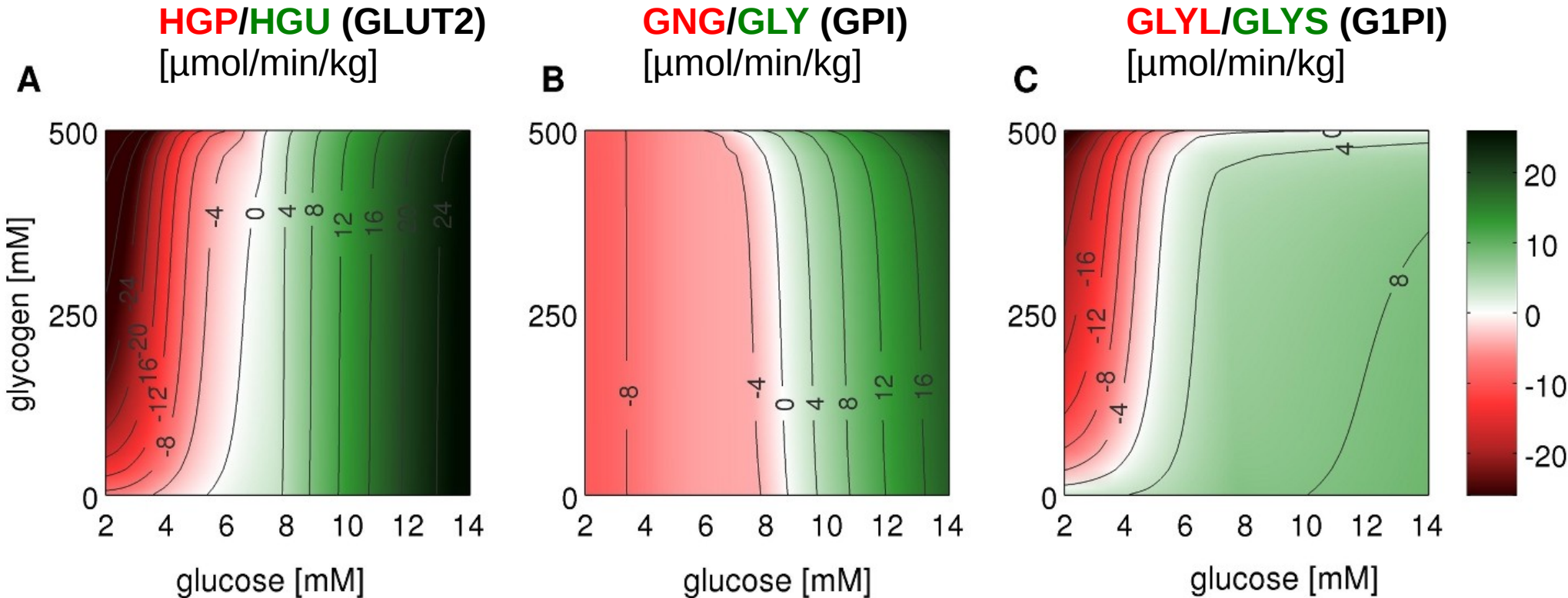
- increase in glycogen postprandial
- depending on glucose concentration between **5mM** and **8mM (7mM)**
- very good agreement with experimental data ([Radziuk2001, Taylor1996, Ferrannini1985])

Simulate glucose metabolism



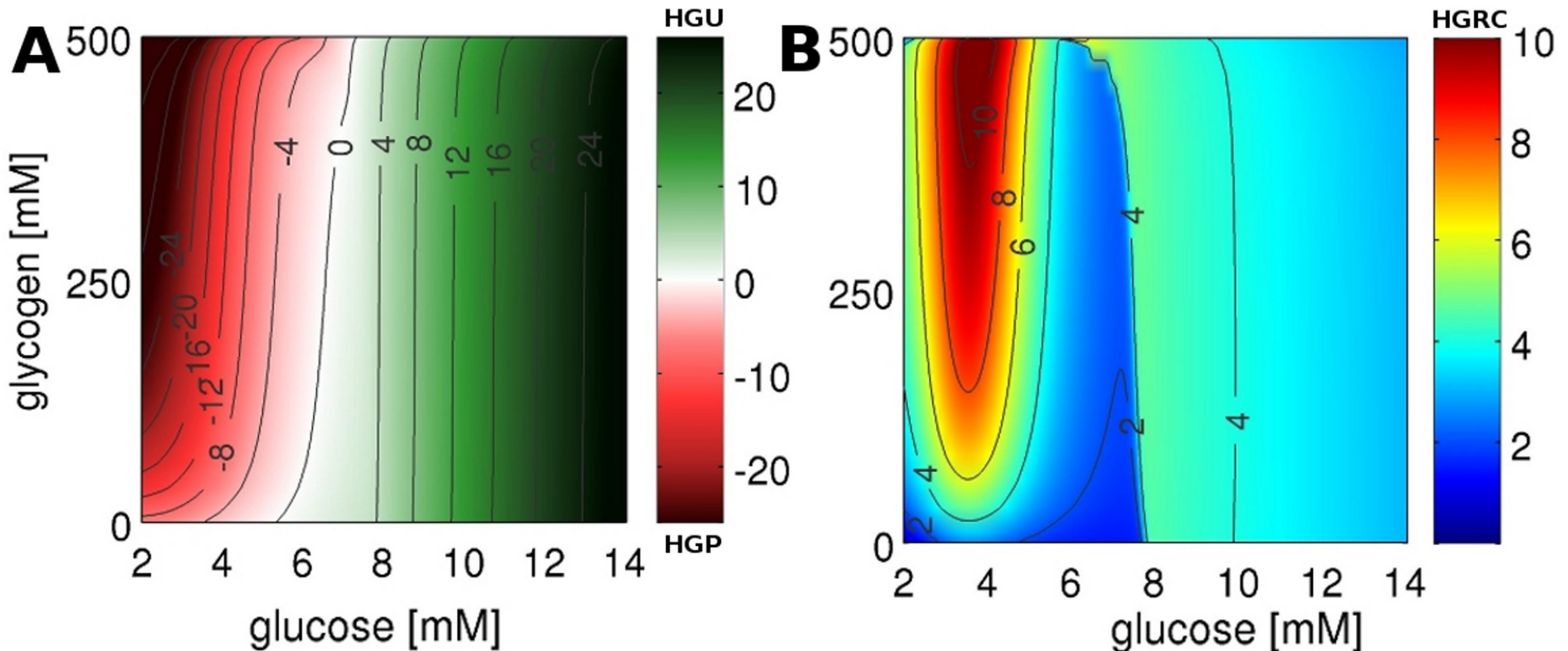
- switch between **HGP** and **HGU** depending on blood glucose
- correct set point of ~6mM
- HGP/HGU fluxes like reported under various conditions
 - postprandial
 - overnight fasting
 - shortterm fasting

Contributions to HGP/HGU



- correct set points
- correct absolute and relative contributions to HGP and HGU under various conditions
 - postprandial, overnight fast, short-term fasting

Liver - A Glucose Homeostate



- ideal regulatory properties to respond to typical physiological challenges to blood glucose homeostasis:
 - hypoglycemia in fasting and muscle activity
 - postprandial hyperglycemia

T2DM (diabetes)

- metabolic disorder characterized by **high blood glucose** in the context of insulin resistance and **relative insulin deficiency**.
- hallmarks are
 - alterations in blood glucose homeostasis
 - increased blood glucose levels
 - increased HGP mainly due to increased gluconeogenesis
- **insulin treatment** standard therapy
 - but associated with hypoglycemic events

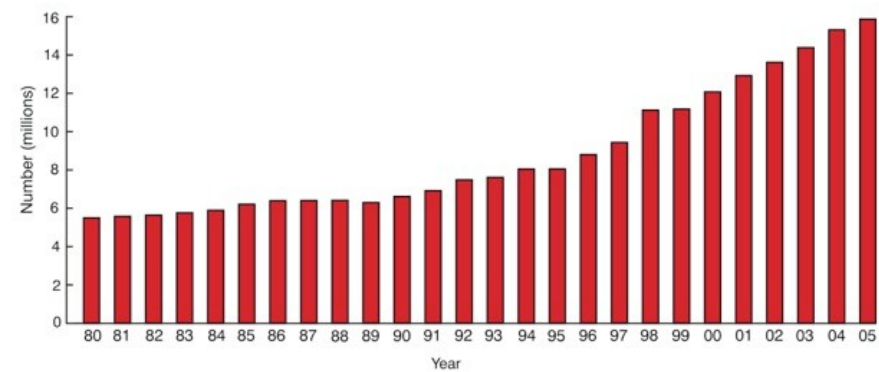
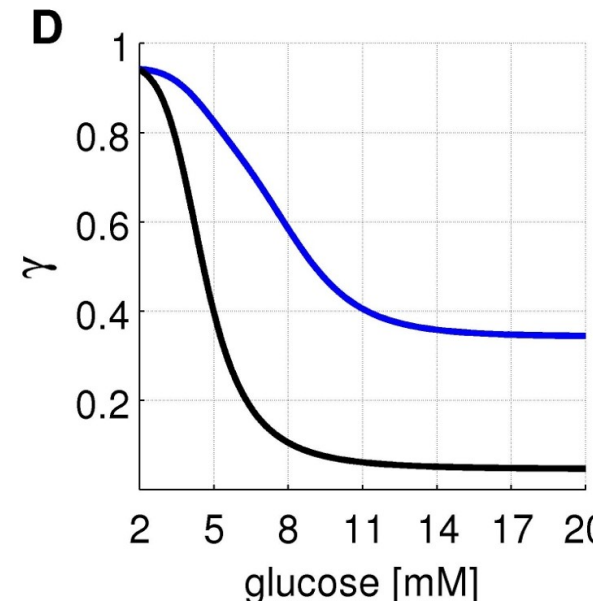
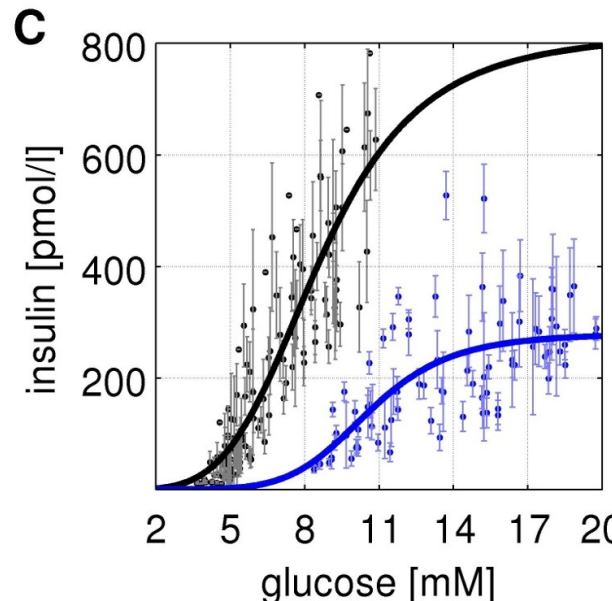
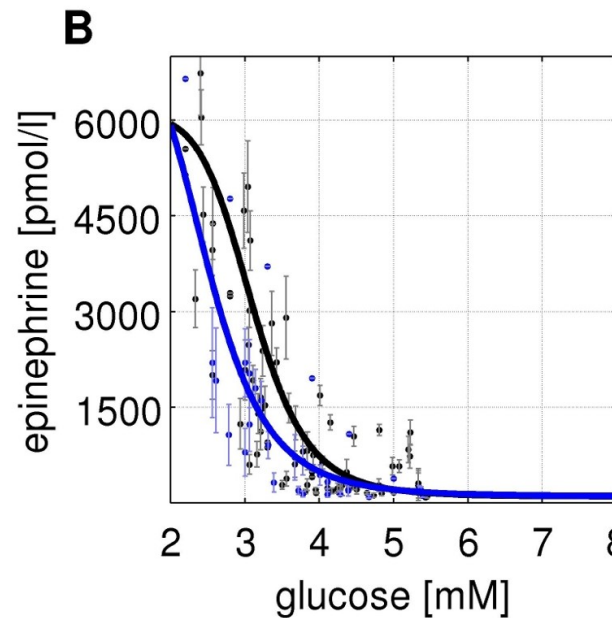
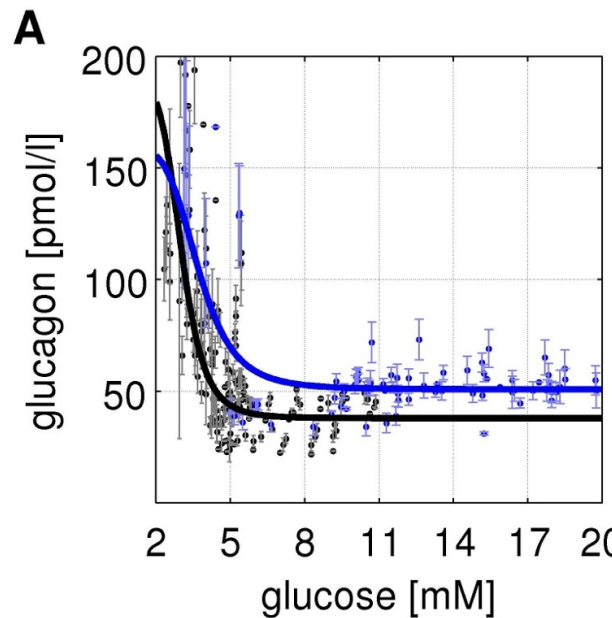


Figure. Increasing prevalence of diabetes.

The prevalence of diabetes has increased at an alarming rate in the United States over the last 25 years and has increased by nearly 5% annually since 1990. According to the Centers for Disease Control and Prevention (CDC), nearly 21 million Americans have diabetes. (Source: CDC)

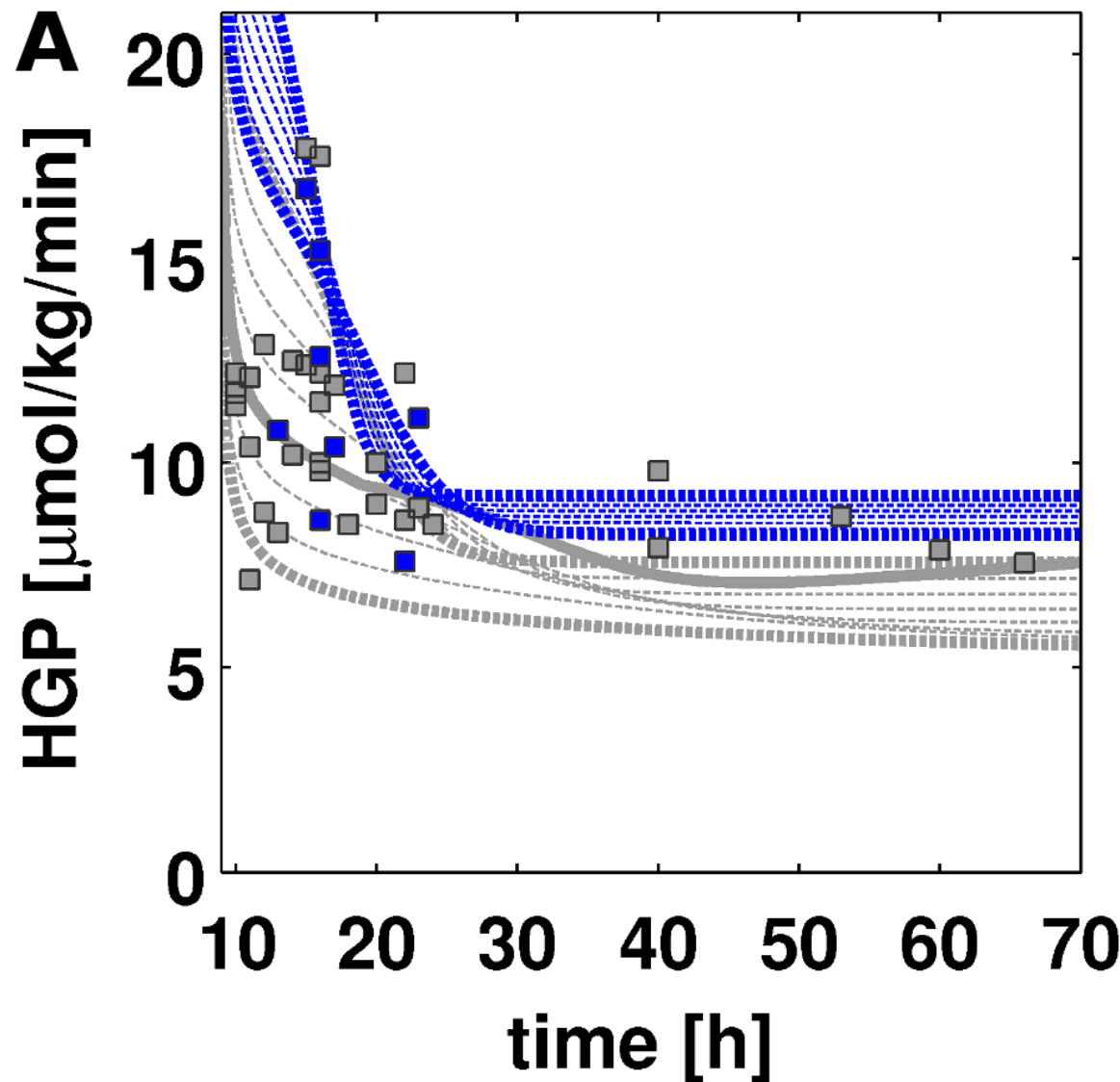


Hormonal responses (T2DM)



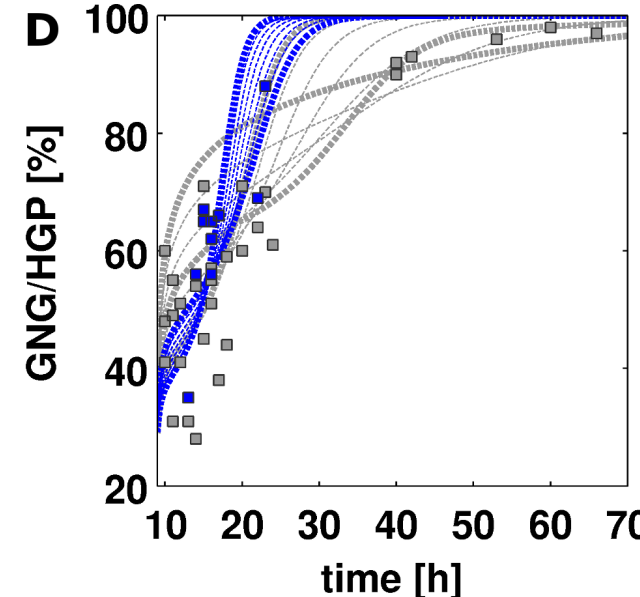
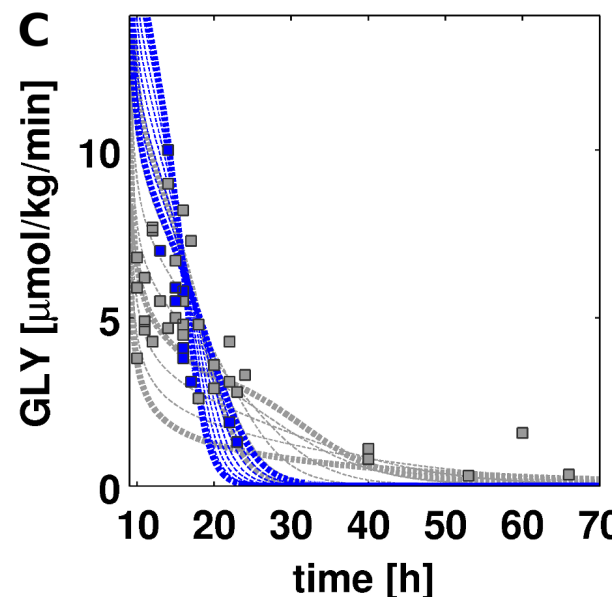
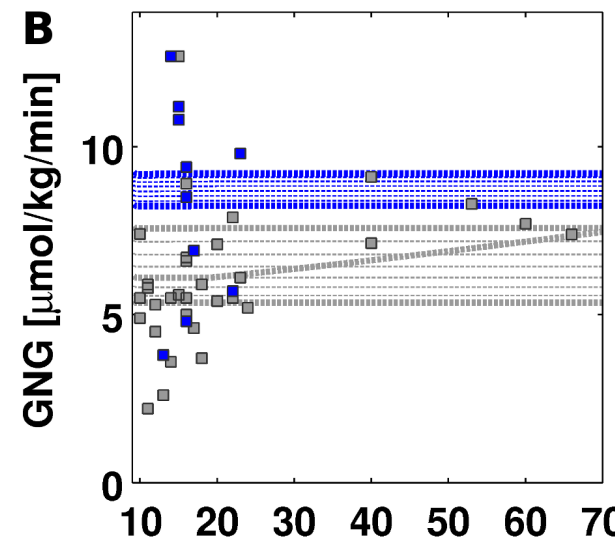
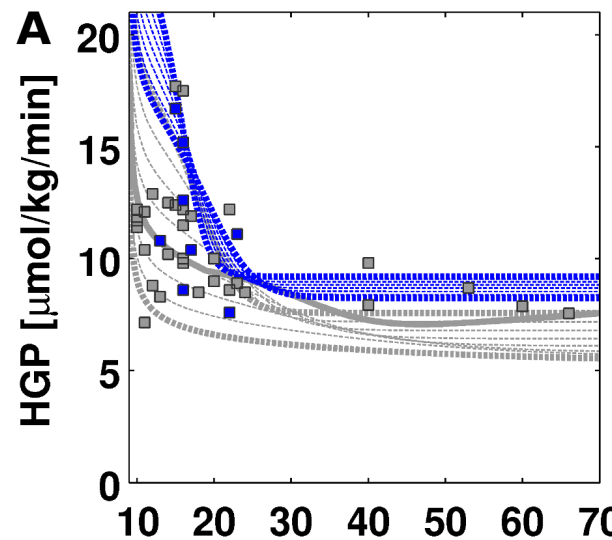
- altered hormonal responses in insulin glucagon and epinephrine
 - **insulin deficiency**
 - **increased basal glucagon**
- phosphorylation state γ is markedly altered
- consequently **glucose metabolism shifted towards a glucose producing phenotype**

T2DM : HGP in Fasting



- increased **HGP** in T2DM
- good prediction of experimental data from a multitude of studies
- no T2DM data used for model fitting !
- model of normal subjects with impaired hormonal responses

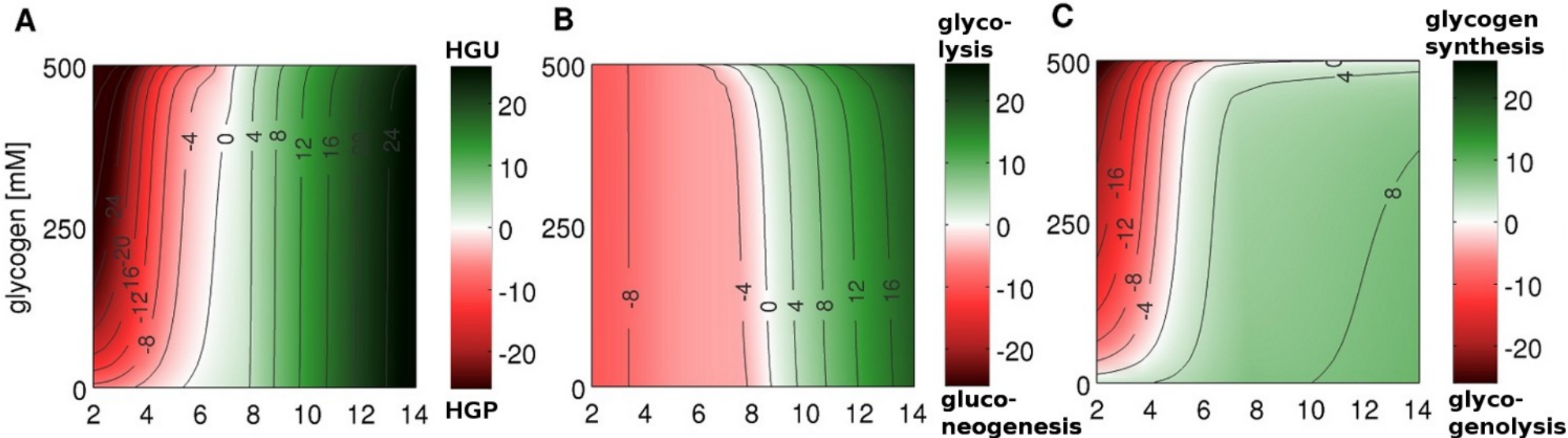
T2DM: Contributions to HGP



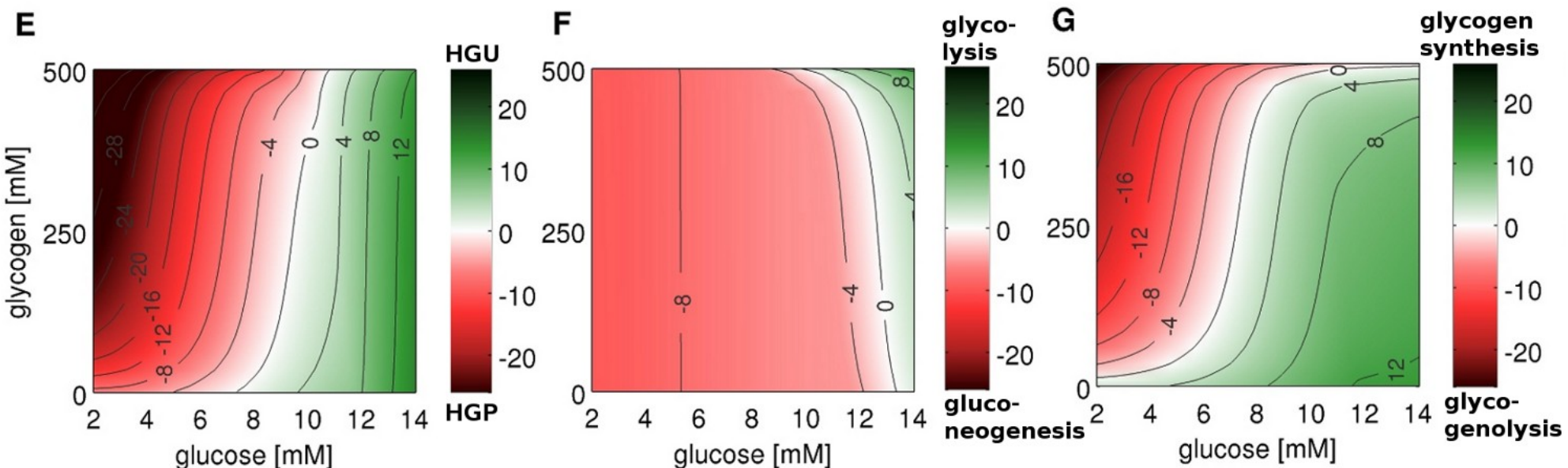
- increased HGP predicted to be mainly due to **increased gluconeogenesis**
- glycogenolysis altered in T2DM
- higher rate and faster decrease in glycogenolysis ($\sim 25\text{h}$ instead of 40h)
- **very good predictions of T2DM phenotype**

T2DM: Shifted metabolism

normal

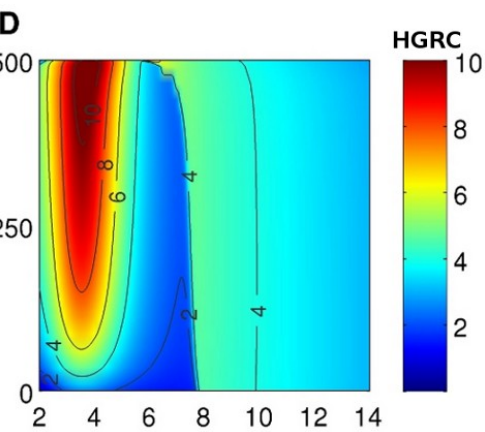
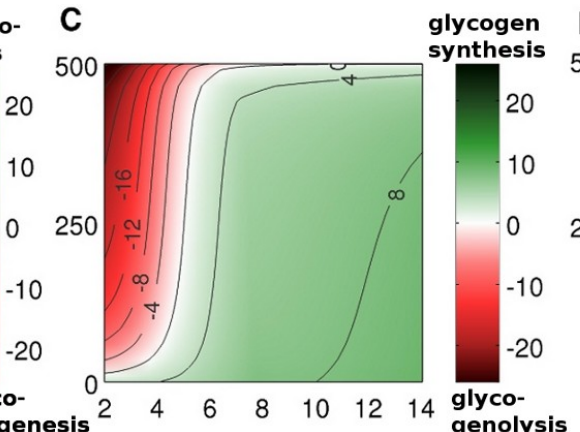
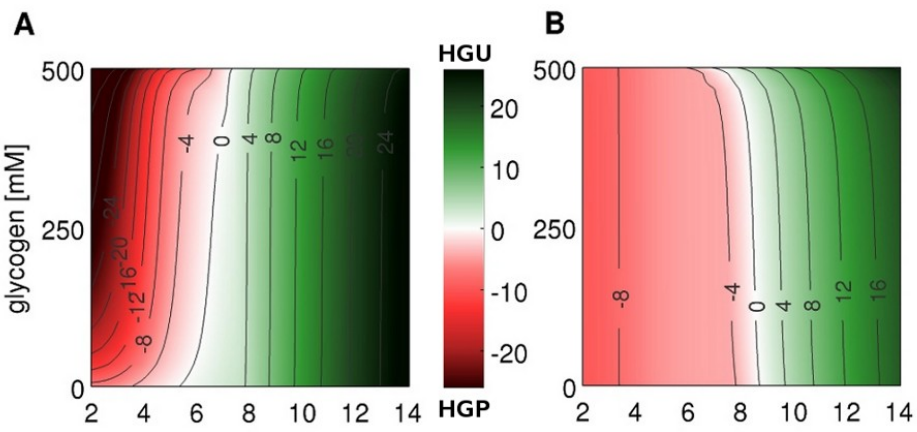


T2DM



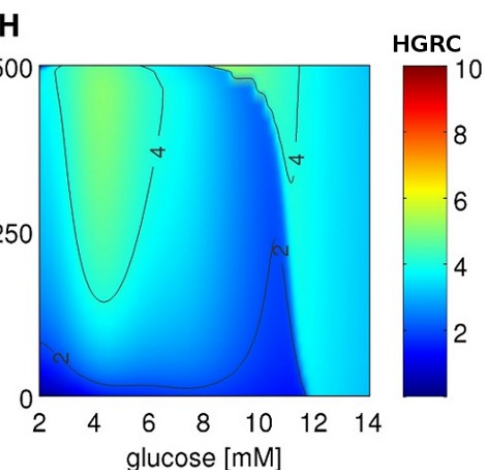
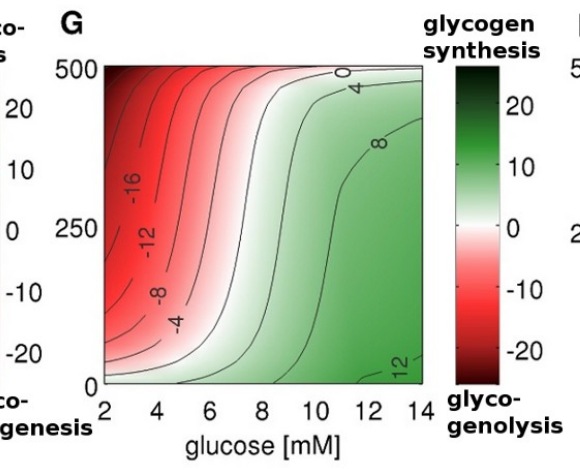
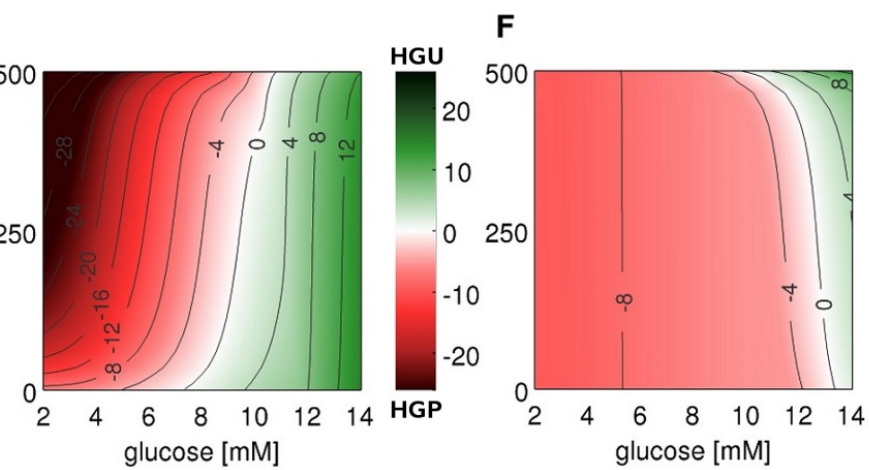
Impaired hepatic response

normal

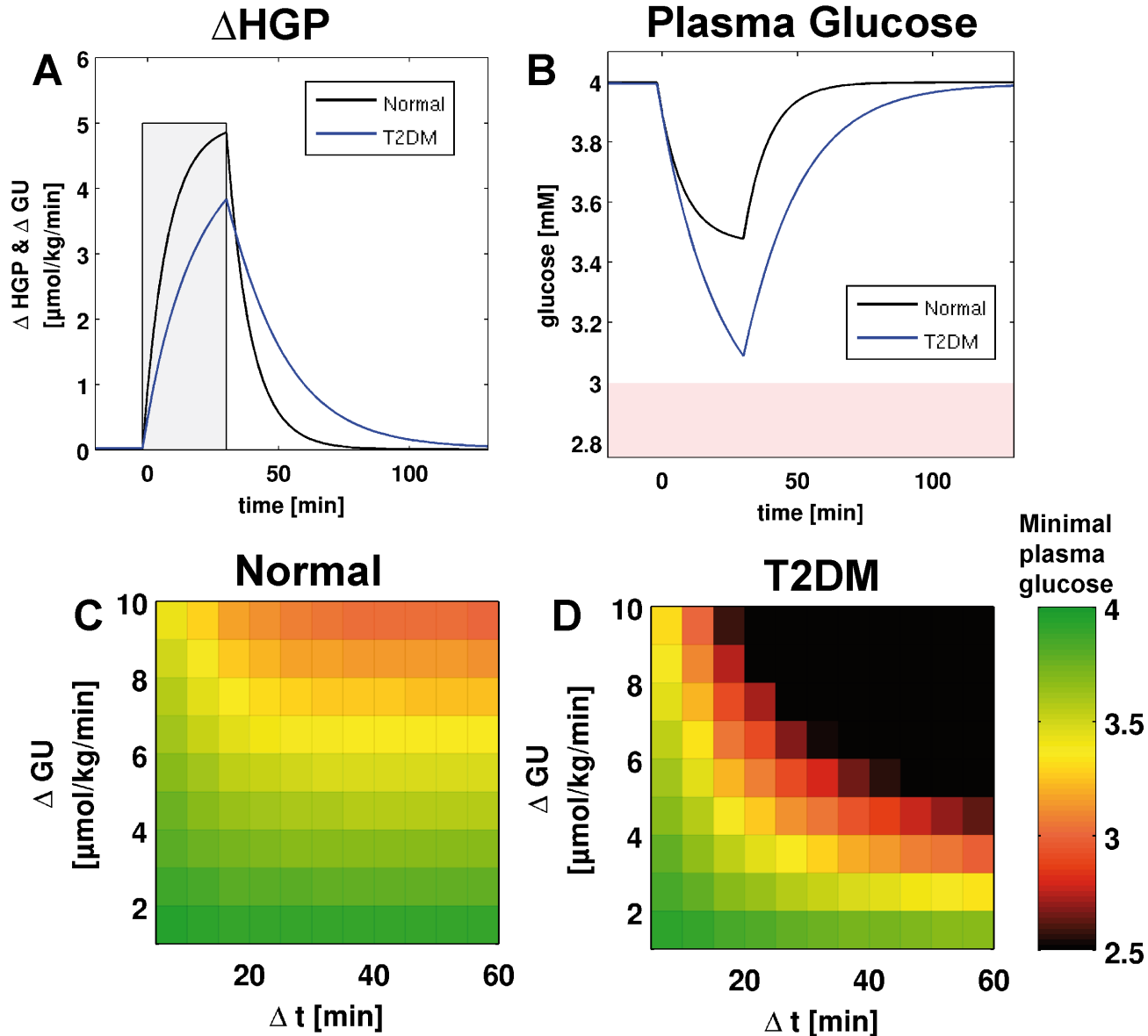


10
8
6
4
2

T2DM



10
8
6
4
2



- hepatic glucose metabolism impaired in T2DM
- reduced capacity for counter-regulation to increase in glucose utilization in T2DM
- **increased risk of hypoglycemic events**

Galactose metabolism & Liver function tests

König M., Holzhütter HG., Berndt N.

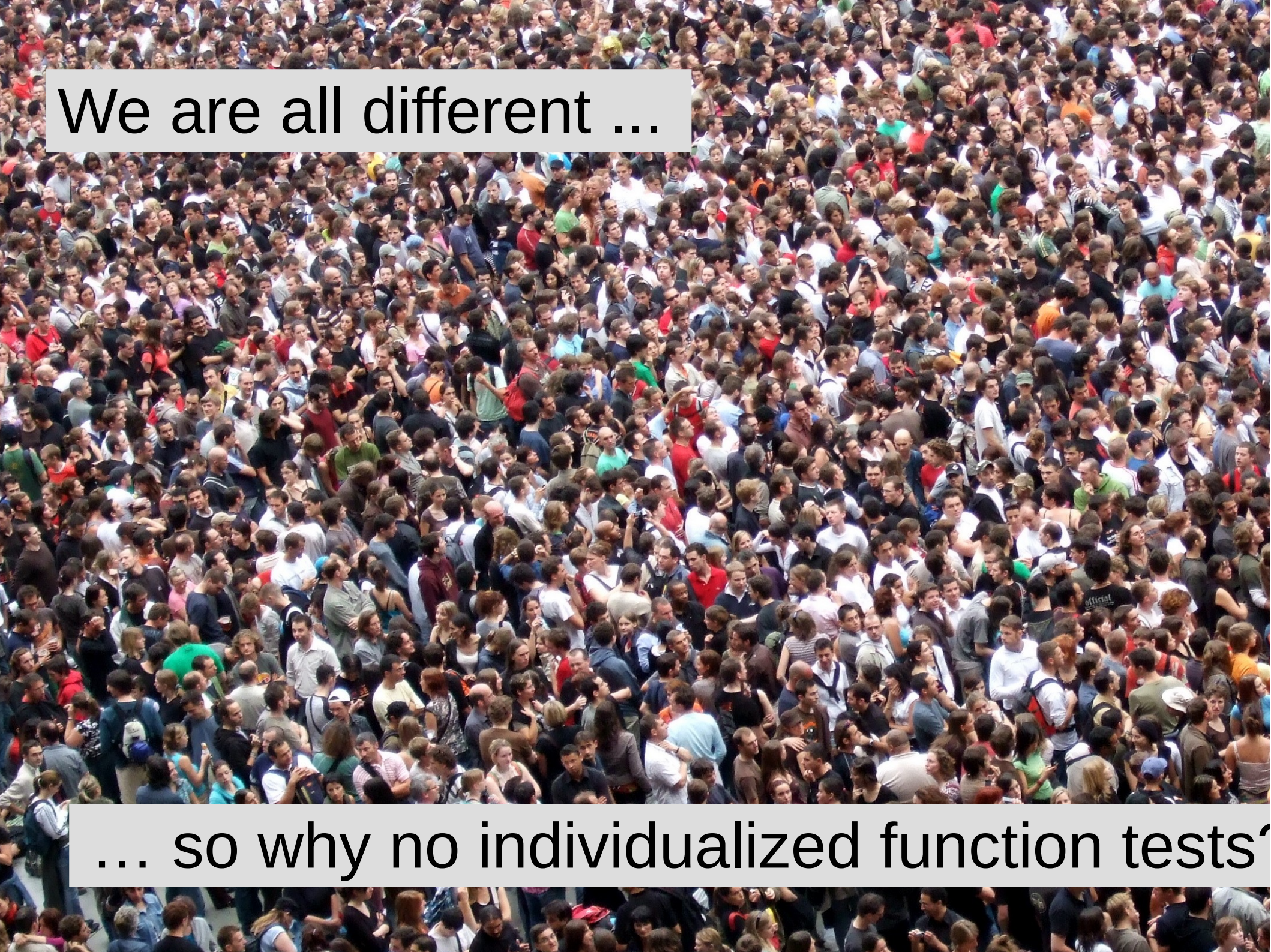
*Metabolic Gradients as Key Regulators in Zonation of Tumor Energy Metabolism: A
Tissue-scale Model Based Study.*

Biotechnol J. 2013 Apr 16.

König M., Marchesini G., Vilstrup H., and Holzhütter HG.

*A Multiscale Computational Model Predicts Human Liver Function From Single-Cell
Metabolism*

2015, [in submission]

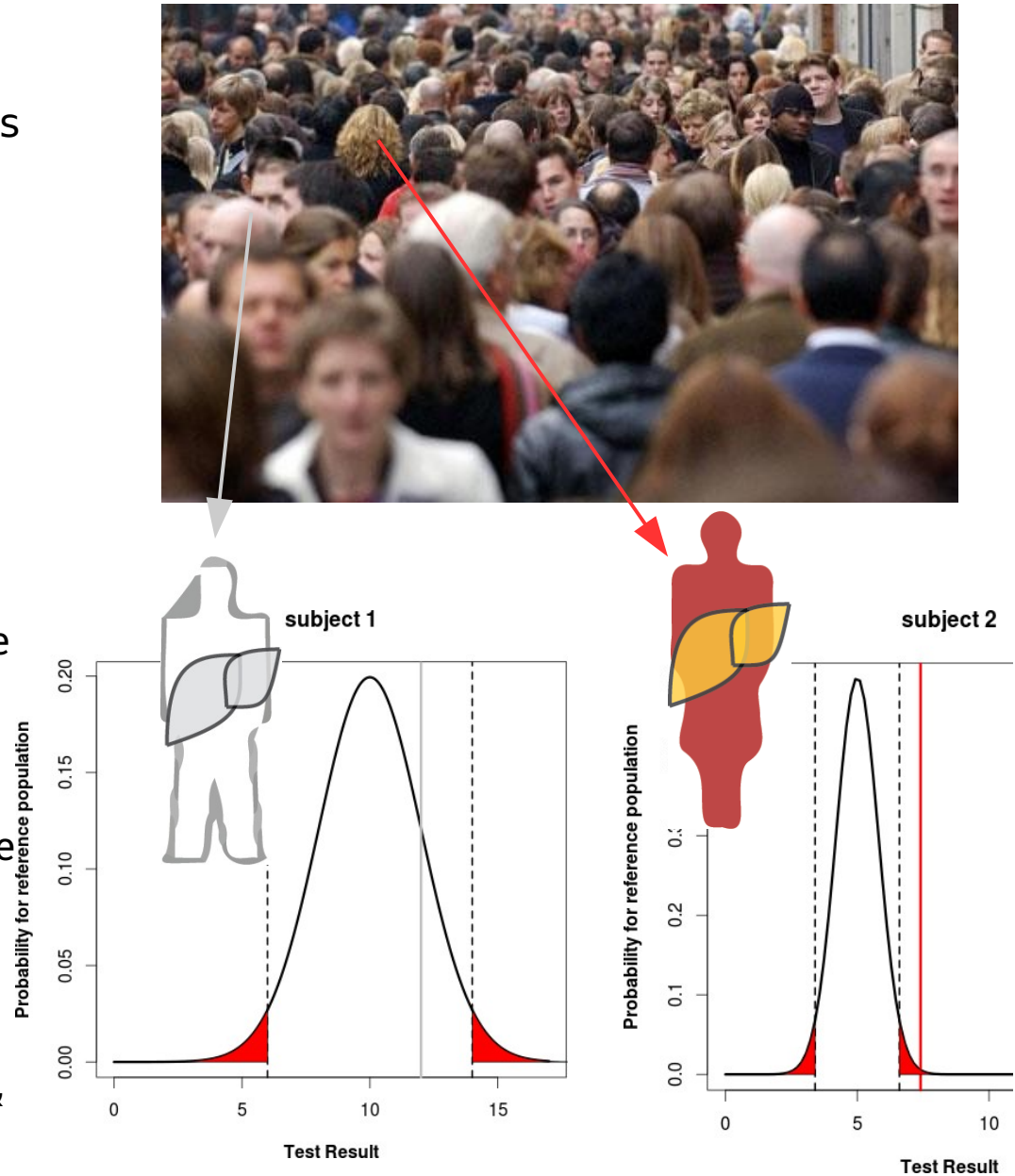
A high-angle photograph of a massive crowd of people, showing a dense assembly of individuals from various backgrounds and ethnicities.

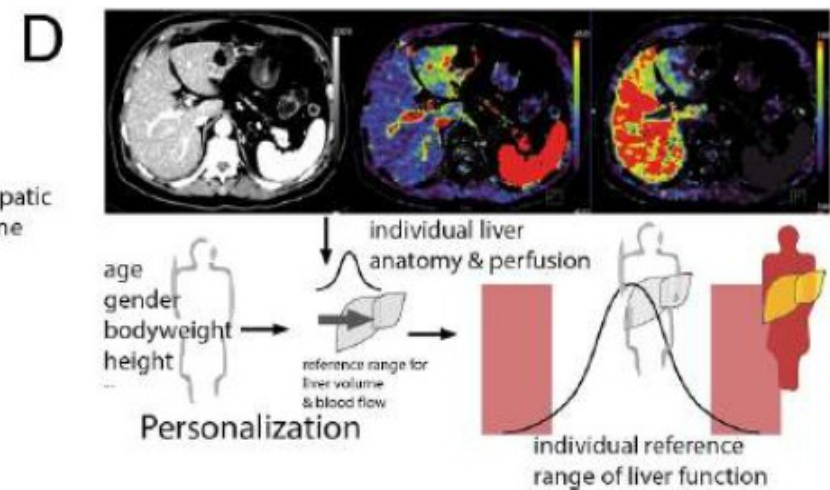
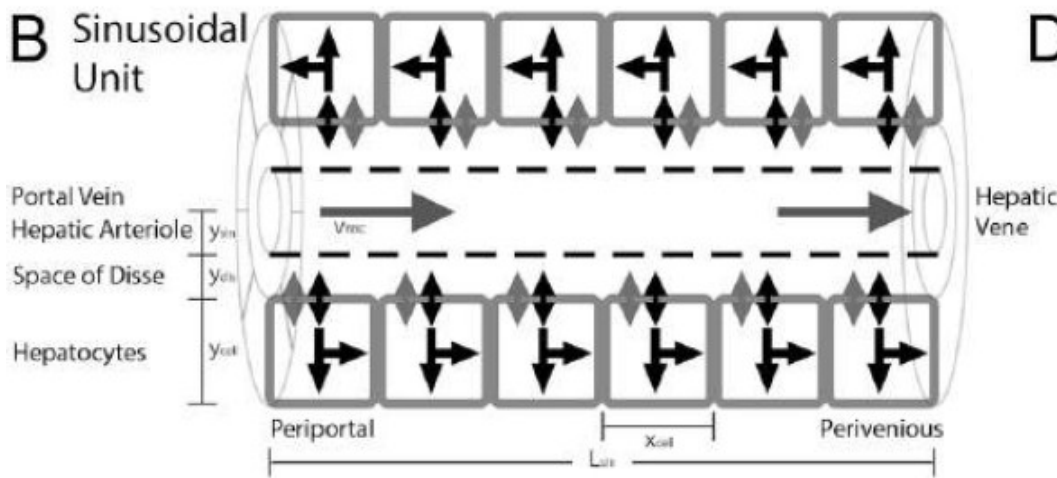
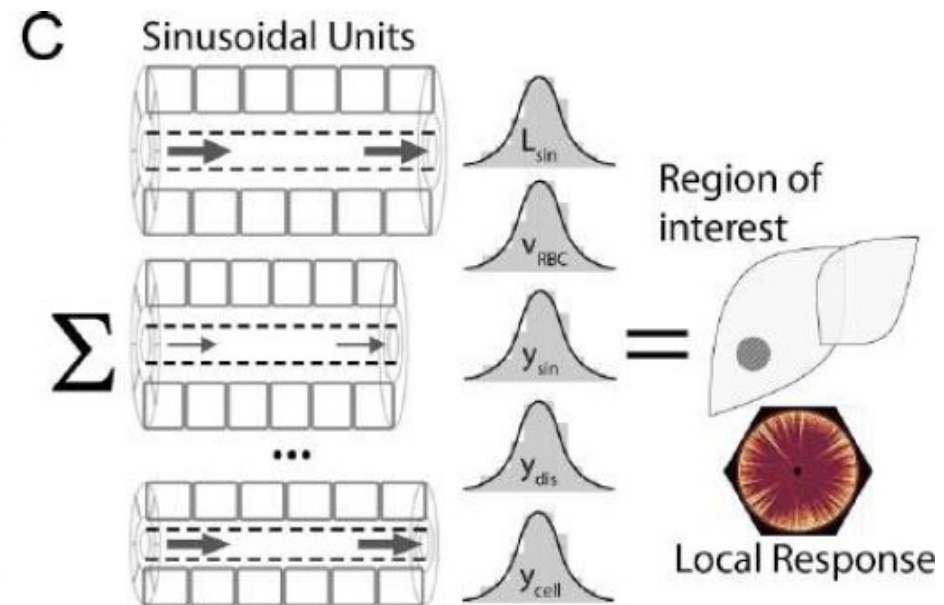
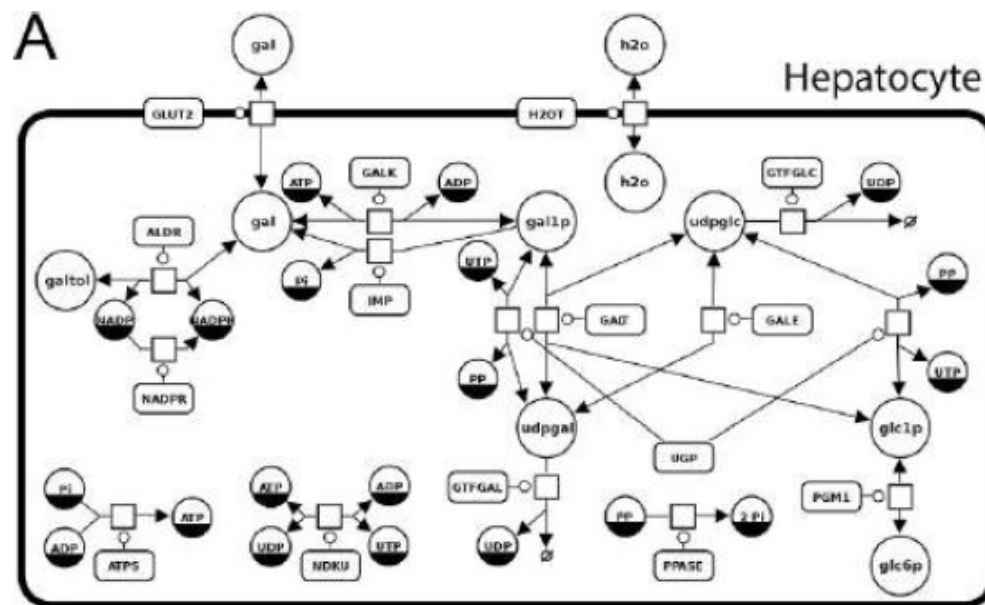
We are all different ...

... so why no individualized function tests?

Liver Function Tests

- Liver is central organ for whole-body metabolism & clearance of galactose
- Galactose elimination capacity (GEC) is established clinical test of liver function
 - Analysis via simple cutoff
 - **But:** large population variability in liver volume & hepatic blood flow
(Age, gender, bodyweight, height, ethnicity, ...)
- **Idea:** Improved evaluation of liver function based on anthropomorphic data & multiscale modelling
 - Individualized liver function test
 - Reference range based on comparable individuals
 - Values outside range → further investigation & treatment
 - Analysis of perfusion, morphological & metabolic effects on liver function

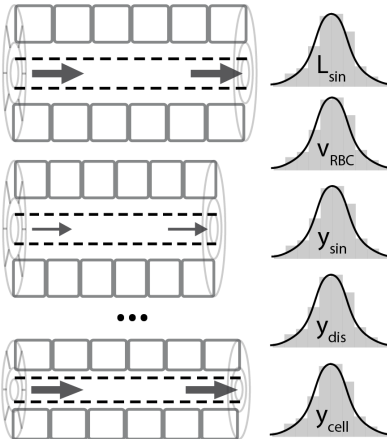




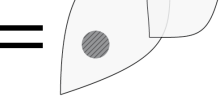
Region of interest

C

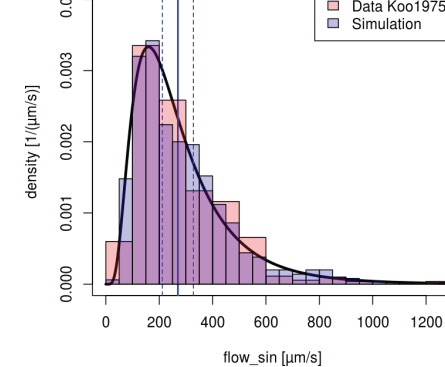
Sinusoidal Units



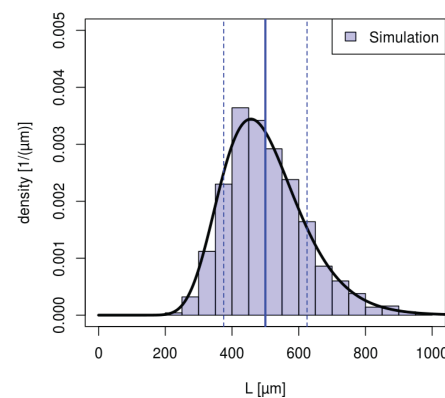
Region of interest



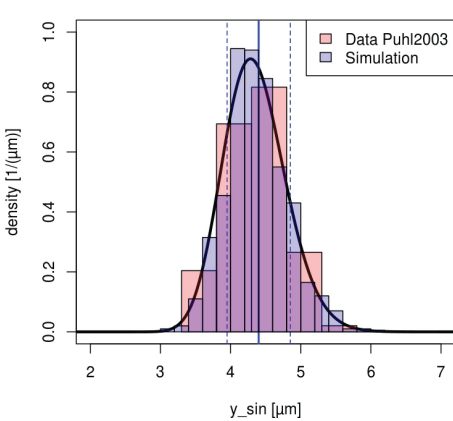
RBC velocity distribution



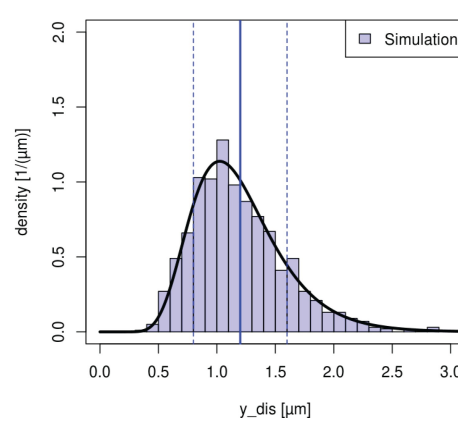
Sinusoidal length



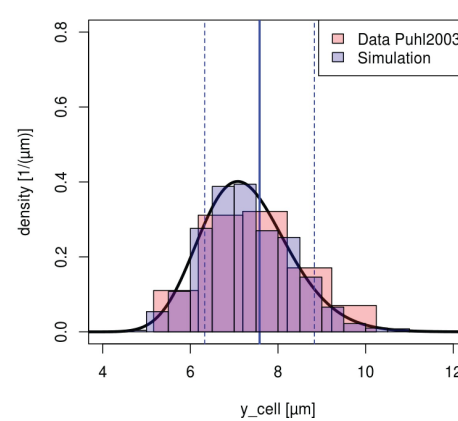
Sinusoidal radius



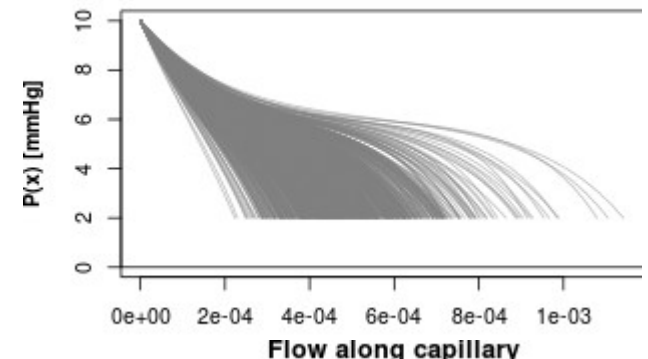
Width space of Disse



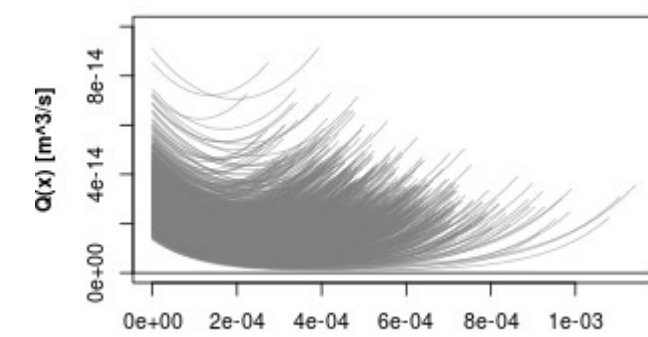
y_cell distribution



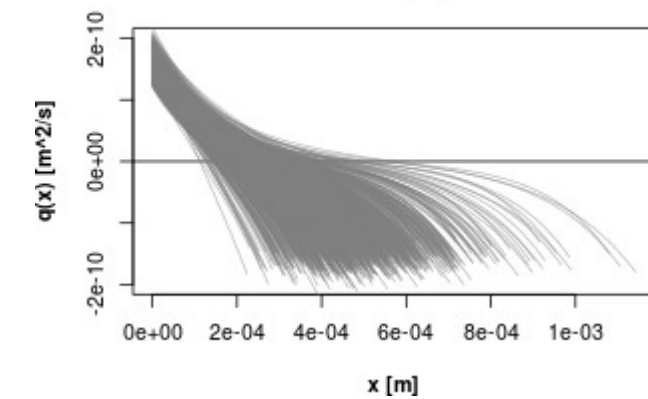
Pressure along capillary



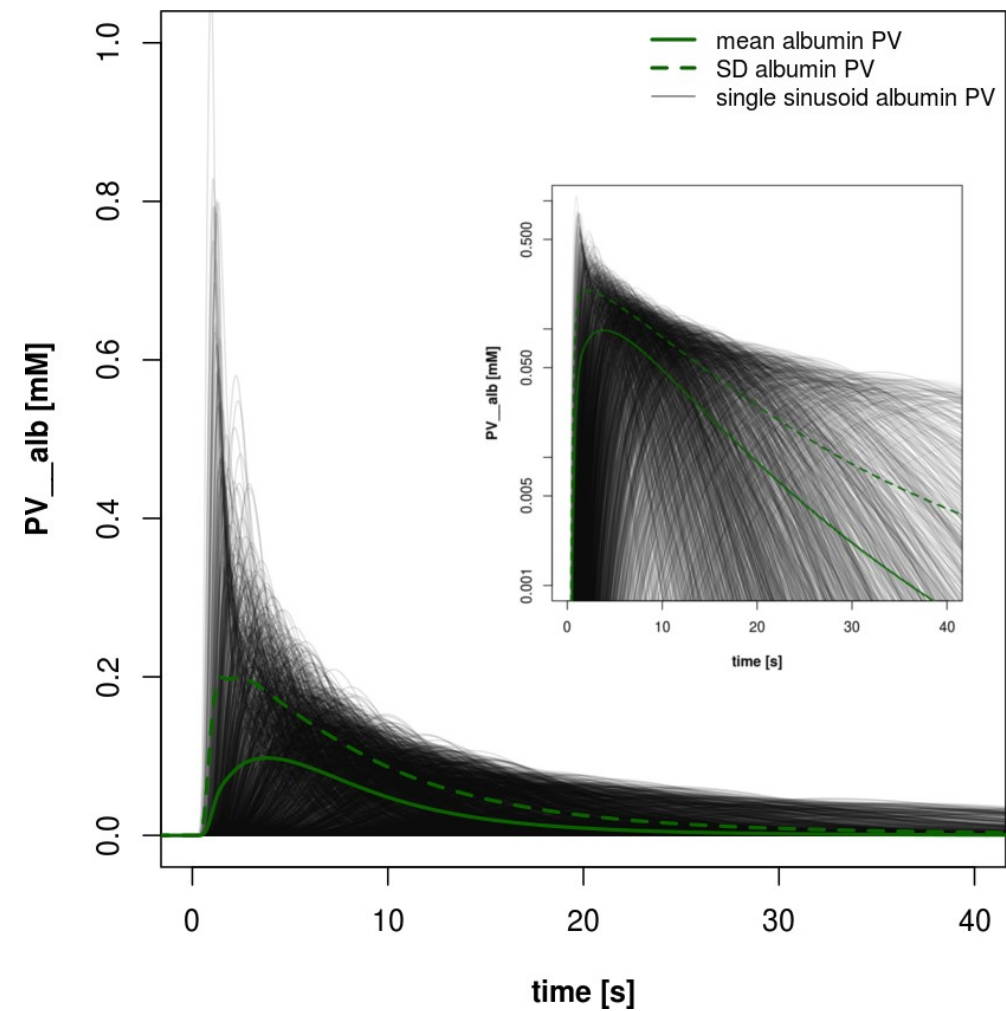
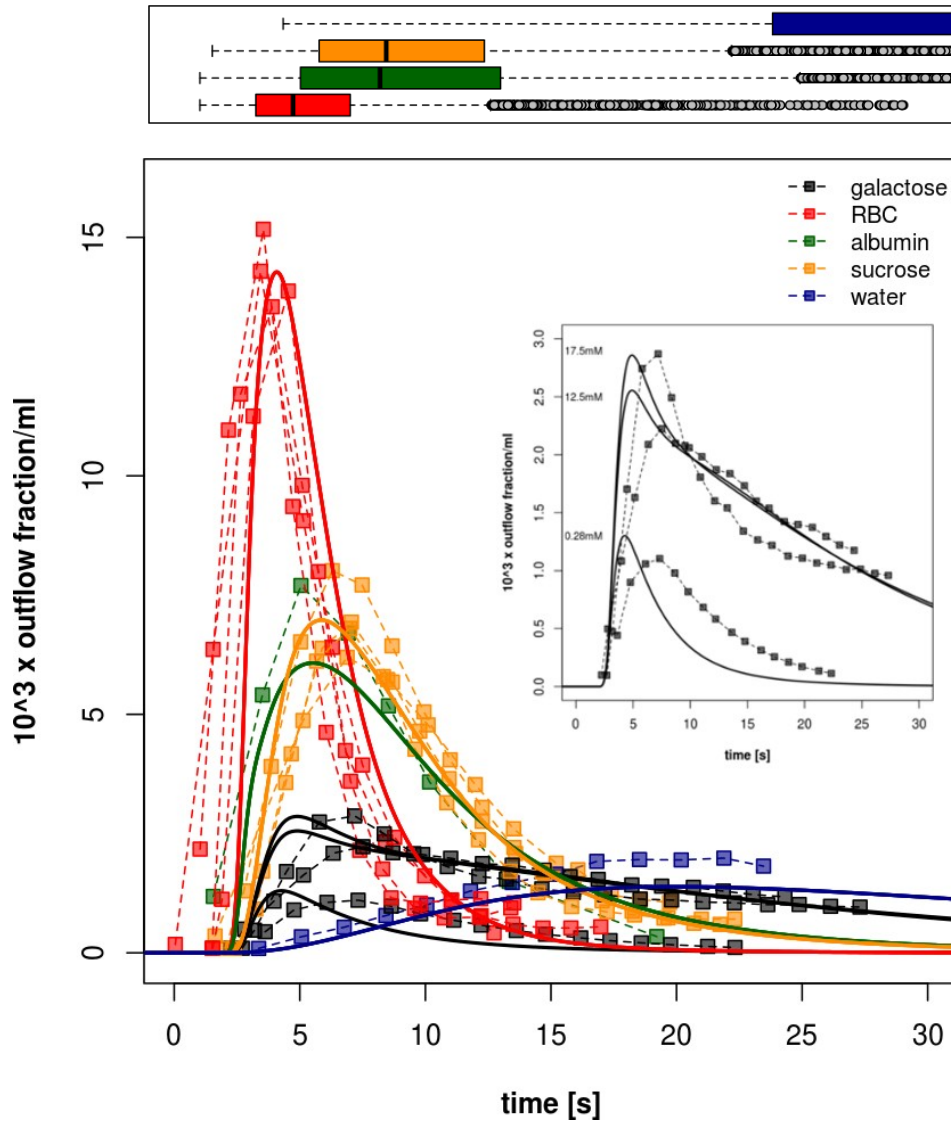
Flow along capillary



Flow through pores



Multiple Indicator Dilution Curves

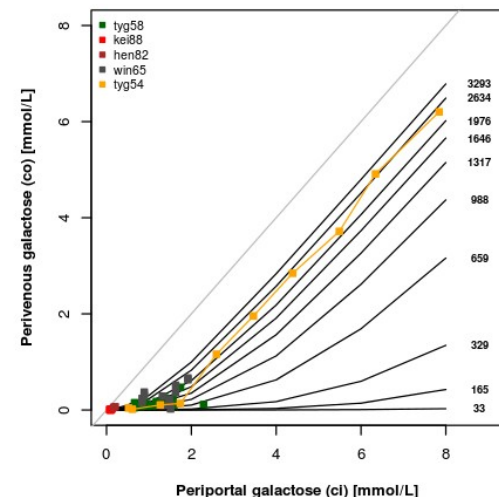
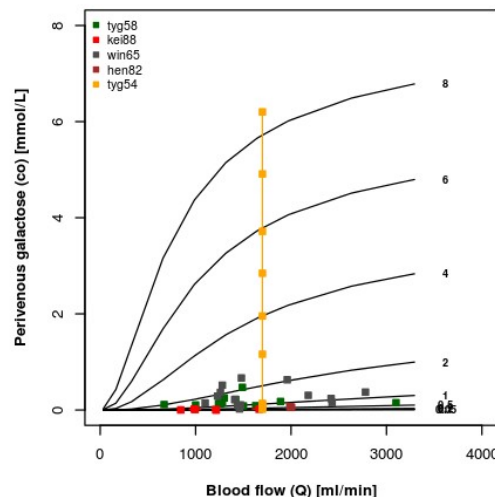
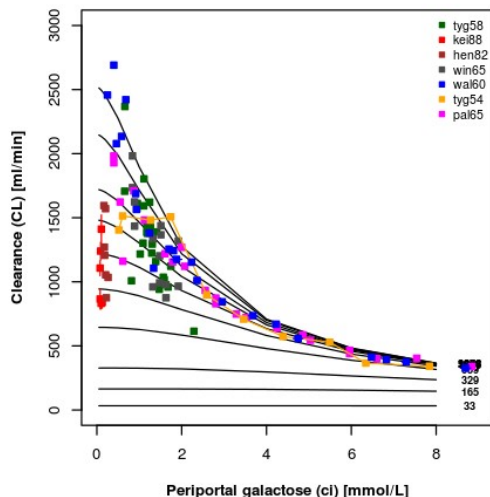
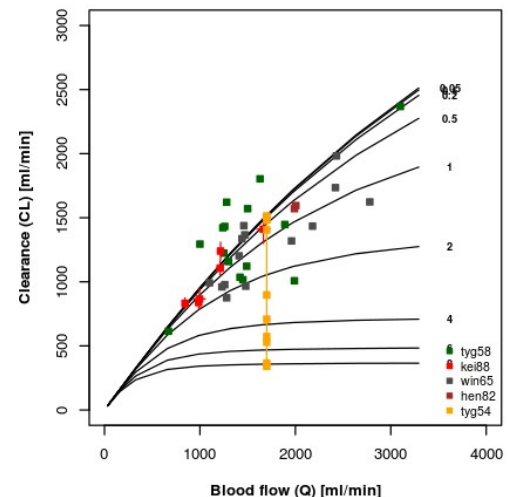
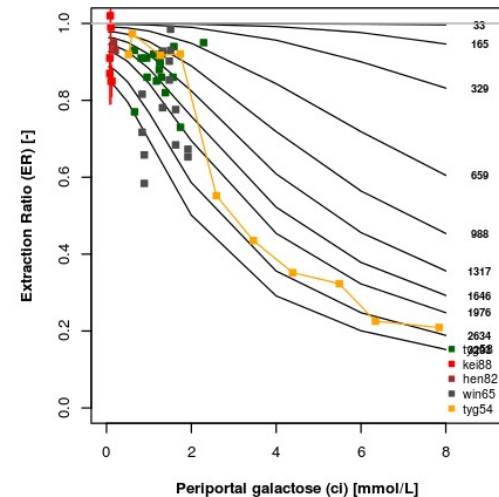
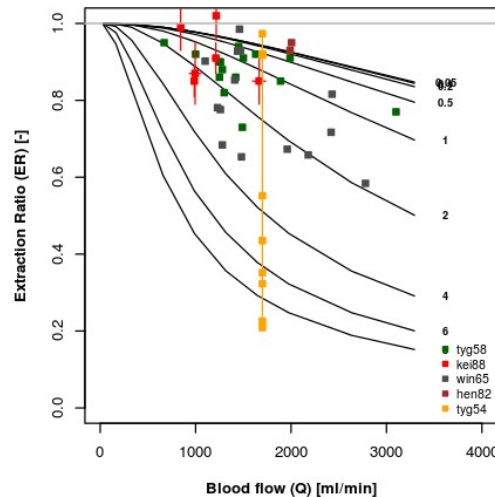
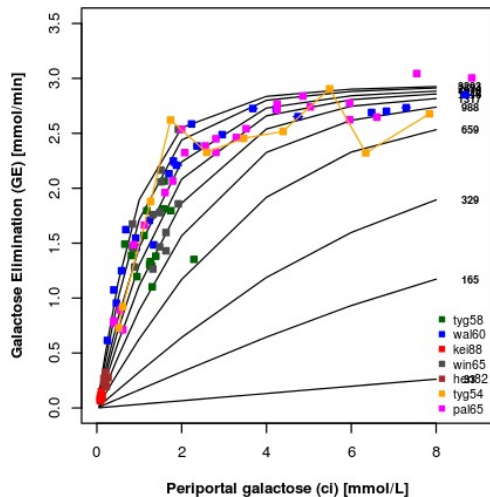
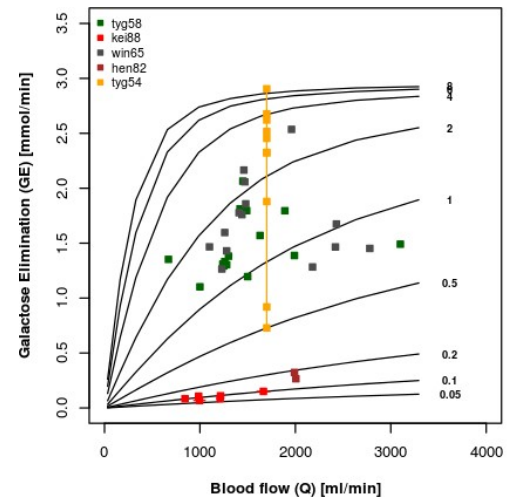


Galactose elimination, extraction ratio & clearance

$$GE[k] = Q_{sin}[k](c_{pp}^{gal}[k] - c_{pv}^{gal}[k])$$

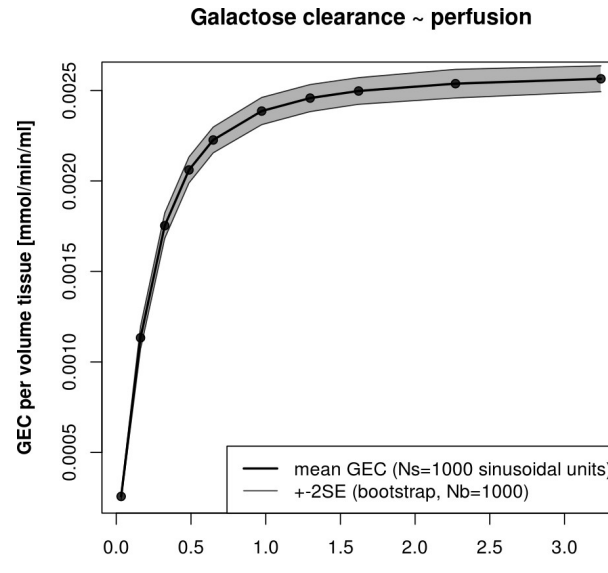
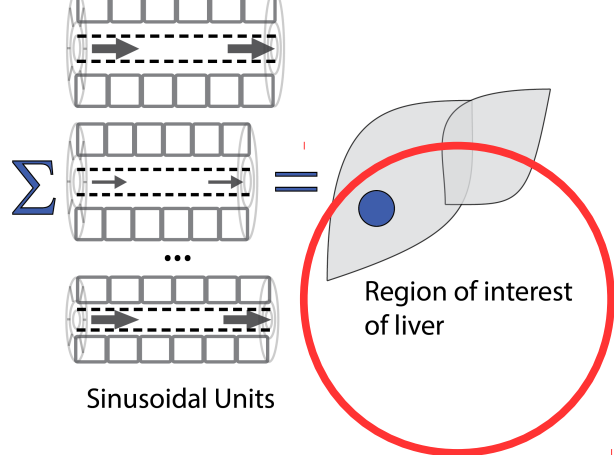
$$ER[k] = \frac{c_{pp}^{gal}[k] - c_{pv}^{gal}[k]}{c_{pp}^{gal}[k]}$$

$$CL[k] = Q_{sin}[k] \frac{c_{pp}^{gal}[k] - c_{pv}^{gal}[k]}{c_{DD}^{gal}[k]} = Q_{sin}[k] ER[k]$$



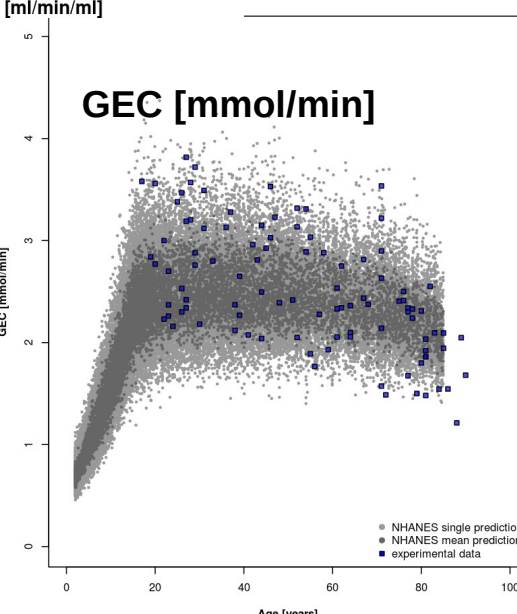
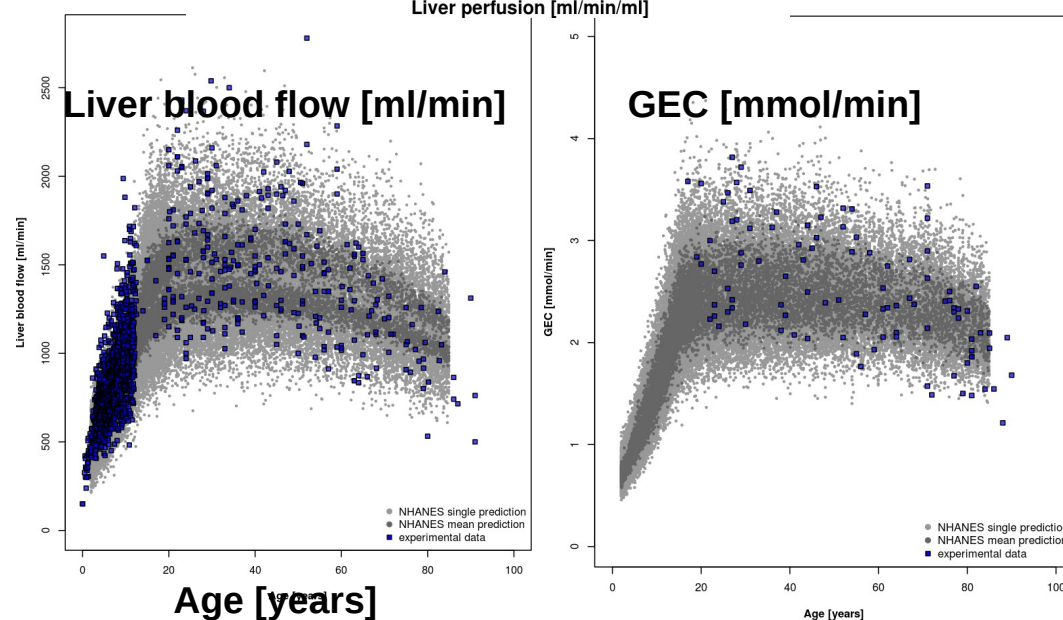
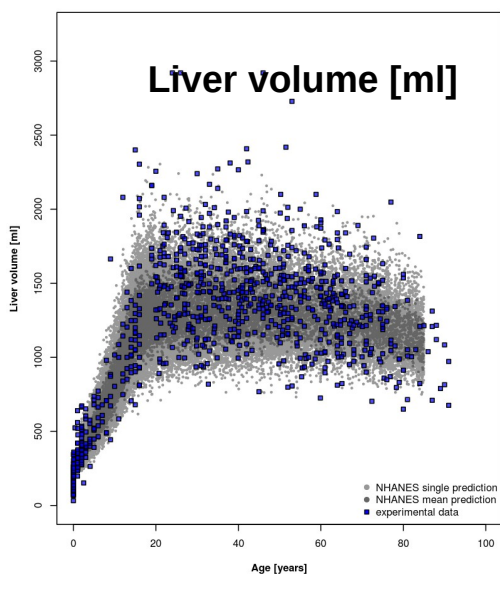
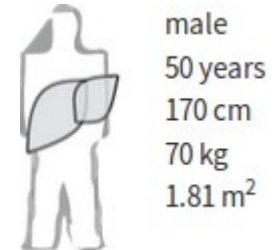
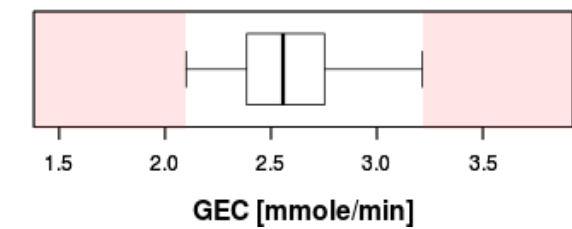
Individualized Liver Function

- Tissue-Model predicts galactose clearance per tissue volume for given perfusion (**regional GEC**)
- Scale with predicted individual distributions of **liver volume and perfusion** (**total GEC**)



GEC Reference Range [2.5% - 97.5%]

[2.10 - 3.21] mmole/min
median 2.56



GEC App

Personalized prediction



Galactose Elimination Capacity (GEC)

Gender

male

Age [years]

50

Height [cm]

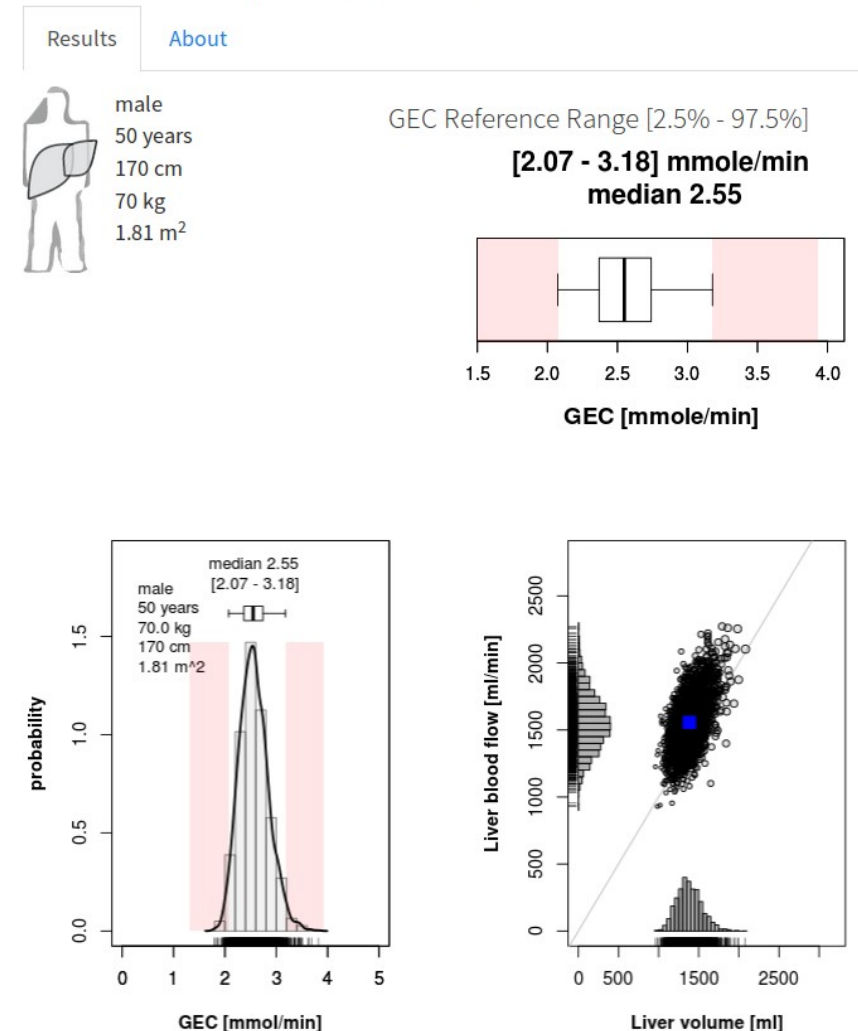
170

Bodyweight [kg]

70

GEC [mmole/min]

Calculate



https://www.livermetabolism.com/gec_app/

Ultrastructure in aging

- **Pseudocapillarization**

- Endothelial cells are thickened and defenestrated with old age

Human		
fenestration radius $\frac{r_{fen}^{old}}{r_{fen}^{young}}$	1.0 old (60 years)/young (20 years)	diameter 58±1nm (young, baboon), 70±2nm (old, baboon), old/young 1.21
porosity $\frac{f_{fen}^{old}}{f_{fen}^{young}}$	0.25 old (60 years)/young (20 years)	porosity determined by scanning electron microscopy 4.2±0.5% (young, baboon), 2.4±0.4% (old, baboon), old/young 0.61
frequency $\frac{N_{fen}^{old}}{N_{fen}^{young}}$	0.25 old (60 years)/young (20 years) (calculated from changes in r and f)	frequency determined by transmission electron microscopy 7.7±0.7 [1/μm] (young, human), 1.5±0.4 [1/μm] (old, human), old/young 0.19 9.4±0.9 [1/μm] (young, baboon), 5.5±0.7 [1/μm] (old, baboon), old/young 0.58
endothelial thickness $\frac{y_{end}^{old}}{y_{end}^{young}}$	1.75 old (60 years)/young (20 years)	Determined by transmission electron microscopy 165±17nm (human, young), 289±9nm (human, old), old/young 1.75 130±8nm (baboon, young), 186±9nm (baboon, old), old/young 1.43

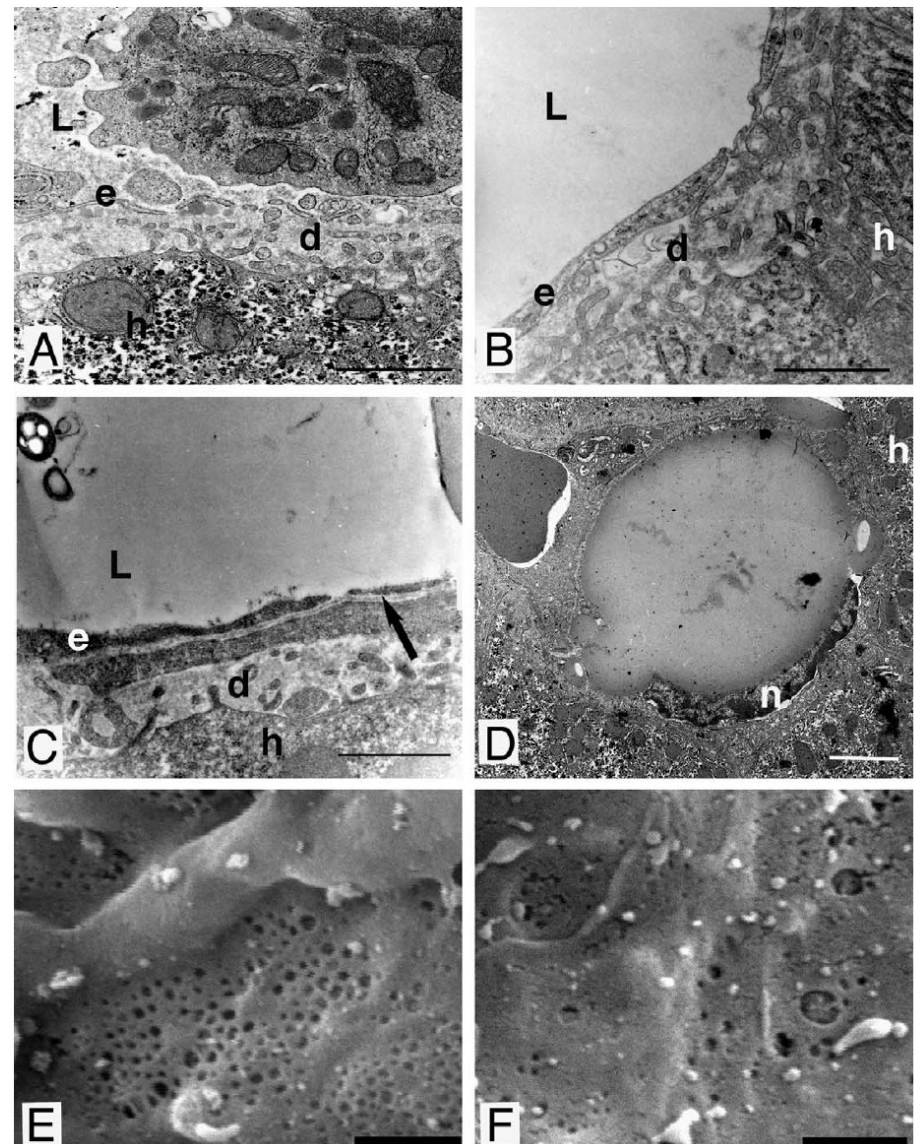
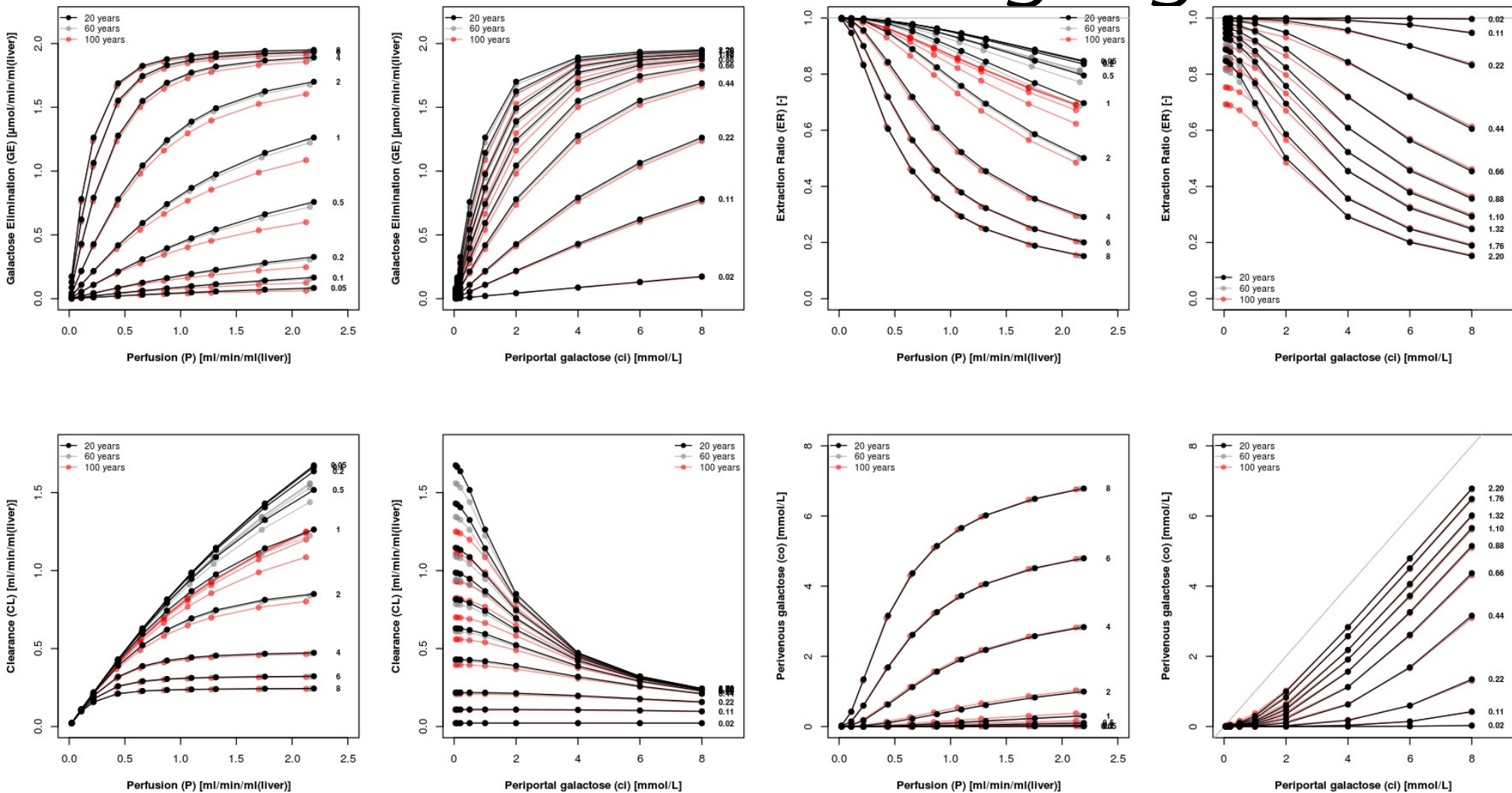


Fig. 2. Electron microscopy of the baboon liver. Transmission electron micrographs of the young (A) and old baboon liver (B–D). The endothelial cells (e) are thickened and defenestrated with old age. Increased extracellular matrix is found in the space of Disse (d) in the old livers. There is basal lamina deposition beneath the endothelial cells in some old baboons (→ (C)). A lipid laden ring-shaped cell is shown in (D). The nucleus (n) is located in the rim of cytoplasm that surrounds the lipid droplet. Scanning electron micrographs of the young (E) and old (F) liver. There is defenstration of the endothelium in the old baboons. (Abbreviations: h, hepatocyte; e, endothelial cell; L, sinusoidal lumen; n, nucleus; d, space of Disse. Scale bars: (A–C, E and F) = 1 μm, (D) = 5 μm).

Alterations in Aging



- Reduced Clearance & Extraction ratio under low concentrations (local effect)
- In combination with reduced liver volume & perfusion in age can have drastic effects on drug/compound clearance

Perfusion heterogeneity (Individuals & liver regions)

Table 2 Liver perfusion showing average of local perfusion rates, and limits of perfusion values obtained from areas $3\cdot5\text{ cm} \times 3\cdot5\text{ cm}$ across liver

Patient	Mean \pm SD (ml/min/100g)	Range
C.B.	58·0 \pm 12·3	35-74
V.B.	60·4 \pm 13·2	34-83
H.H.	68·6 \pm 12·3	52-87
I.H.	70·2 \pm 17·1	40-98
E.M.	97·4 \pm 11·0	77-116
H.M.	101·5 \pm 19·7	69-131
B.P.i.	66·3 \pm 10·3	49-83
B.P.	122·6 \pm 22·2	96-187
N.P.	55·1 \pm 12·1	32-85
F.S.	70·9 \pm 9·9	56-85
G.S.	80·6 \pm 10·3	55-100
L.S.	52·8 \pm 9·2	37-62
M.S.	98·6 \pm 24·9	49-128
N.S.	100·0 \pm 24·0	55-127

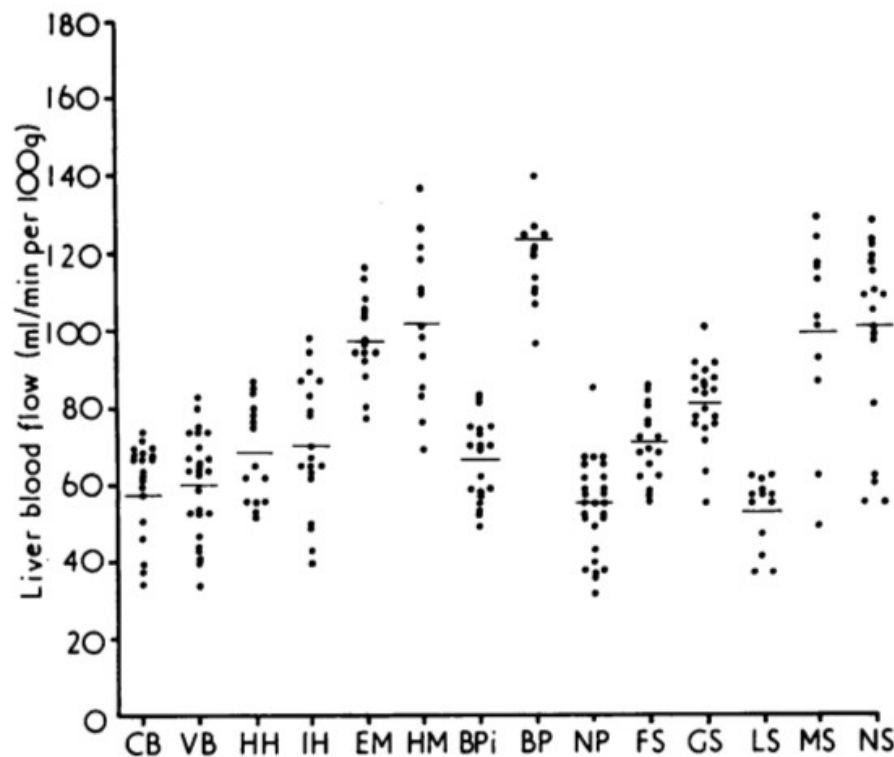
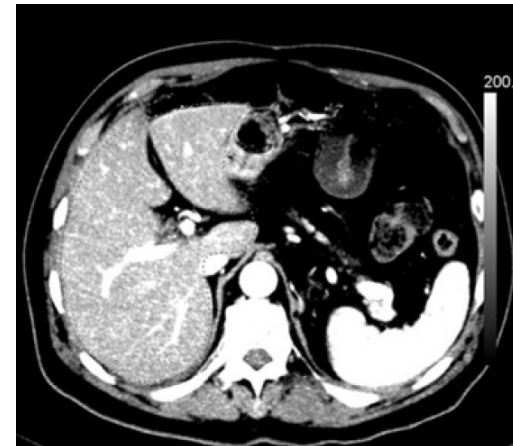


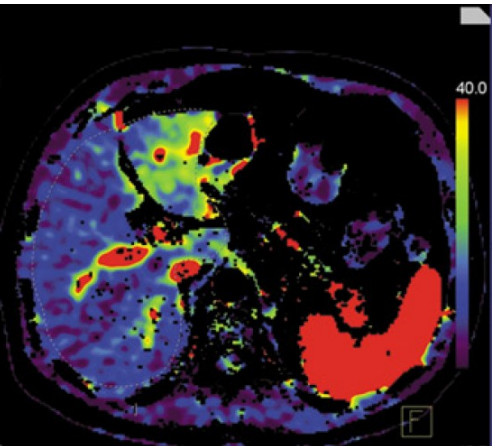
Fig. 2 Distribution of the perfusion rates of each individual element of the liver for each subject to illustrate the wide range of values obtained.

Local galactose elimination

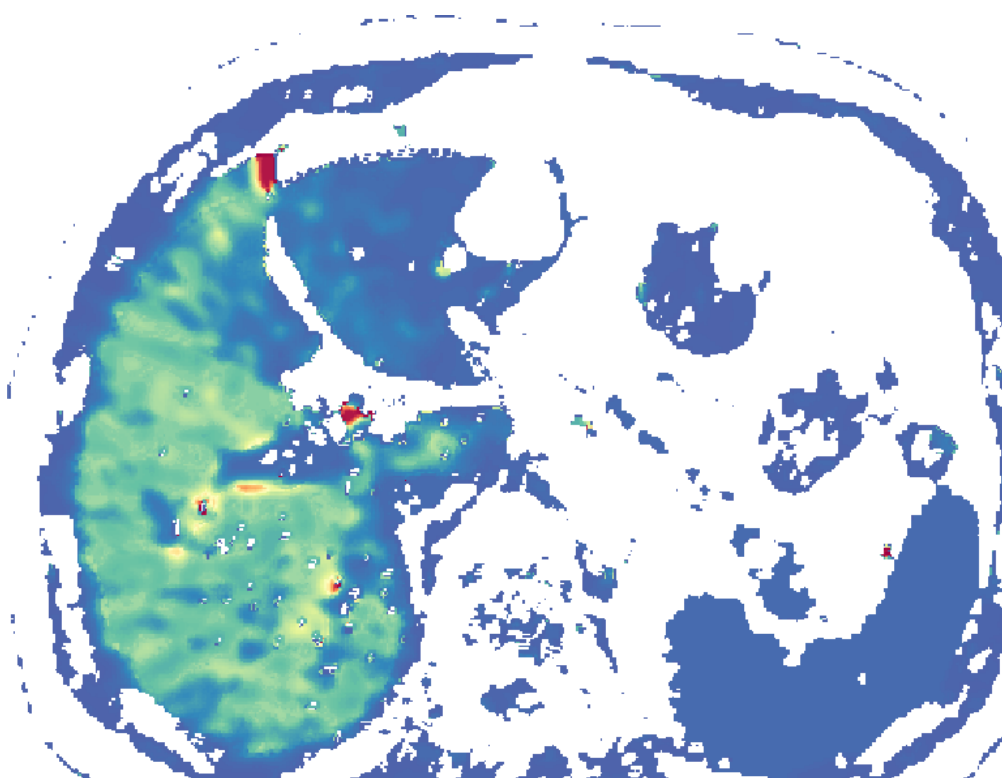
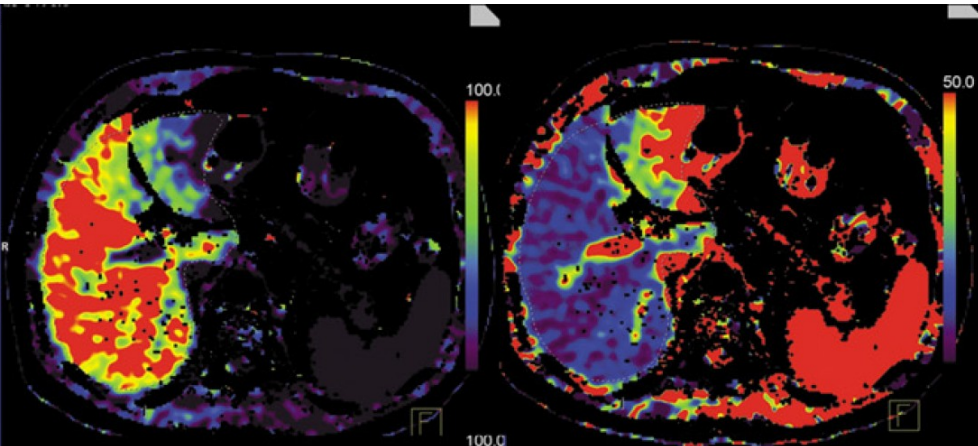
ALP (arterial liver perfusion)



PVP (portal-venous perfusion)



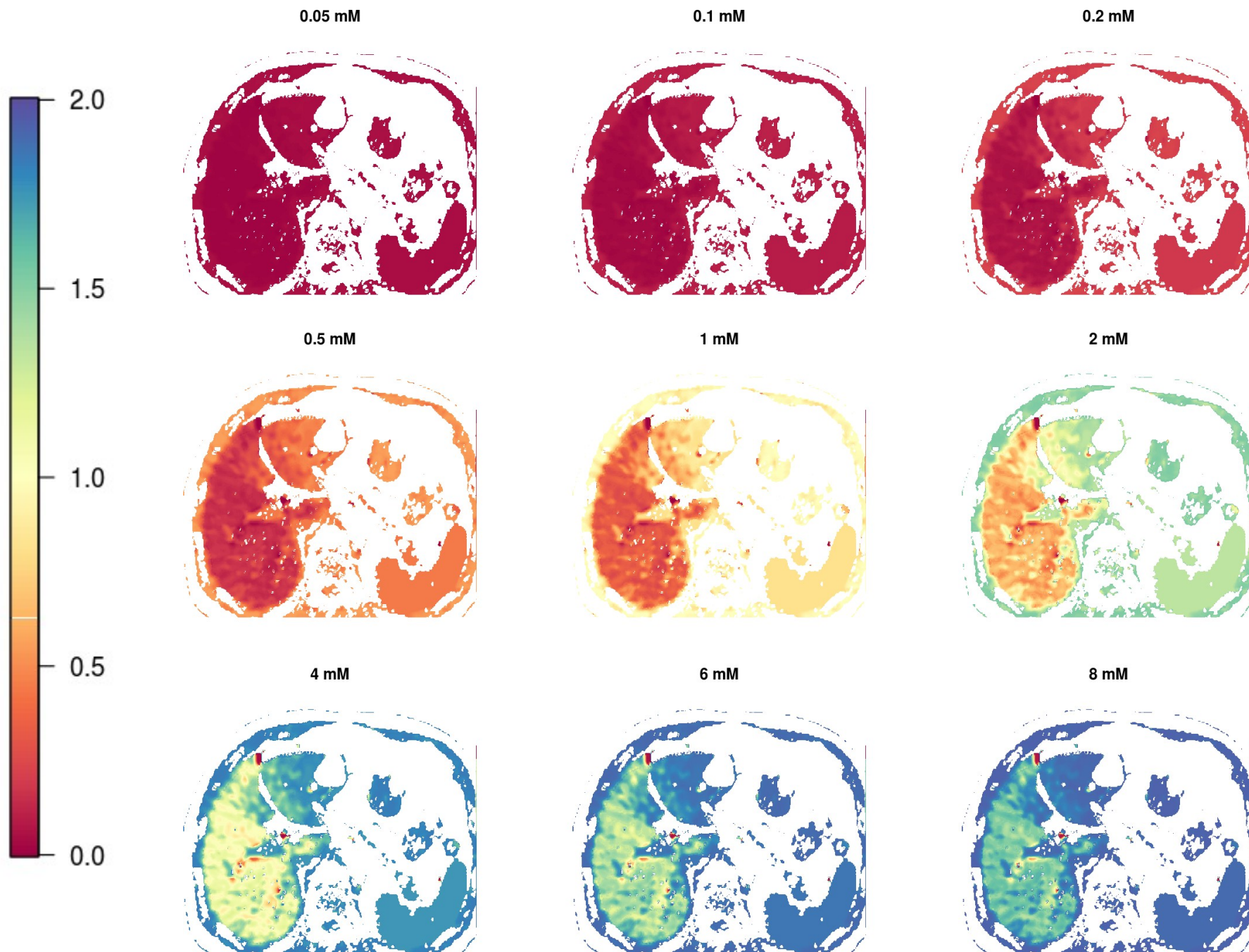
HPI (hepatic perfusion index)



2.0 GE [$\mu\text{mol}/\text{min}/\text{ml(tissue)}$]
Galactose elimination (8mM galactose)

- Galactose elimination depending on local liver perfusion
- THP = ALP + PVP
(total hepatic perfusion)

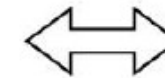
GE [$\mu\text{mol}/\text{min}/\text{ml(tissue)}$]
Galactose elimination depending on galactose



Thank you for your attention

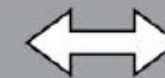
LiSyM – Junior group

WP0 Project Management & Organisation



Central Project Management

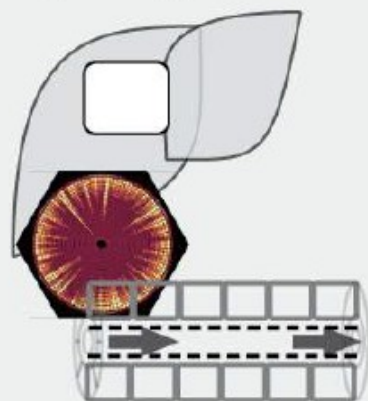
WP1 Standardization & Data Management



Central Data Management

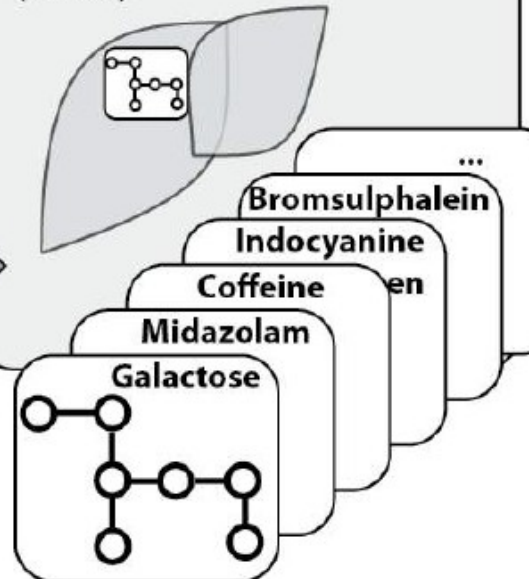
WP2 Multi-scale Model

standardized model (SBML)
template physiology &
morphology



WP3 Metabolic Initialization

model initialization via
standardized submodels
(SBML)



WP4 Personalization & Translation

model individualization
personal liver function
reference ranges
improved function tests

age
gender
bodyweight
height
...

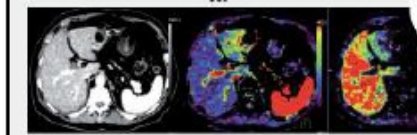
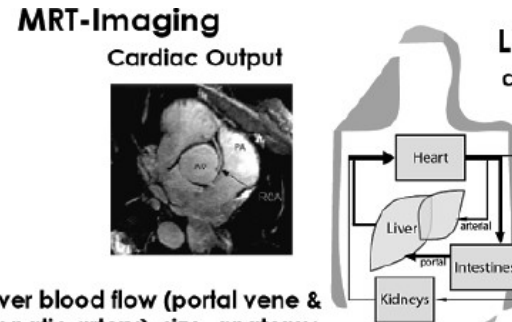
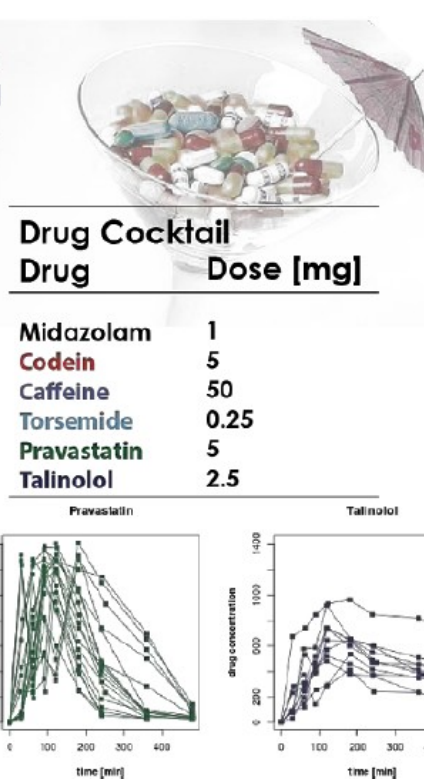
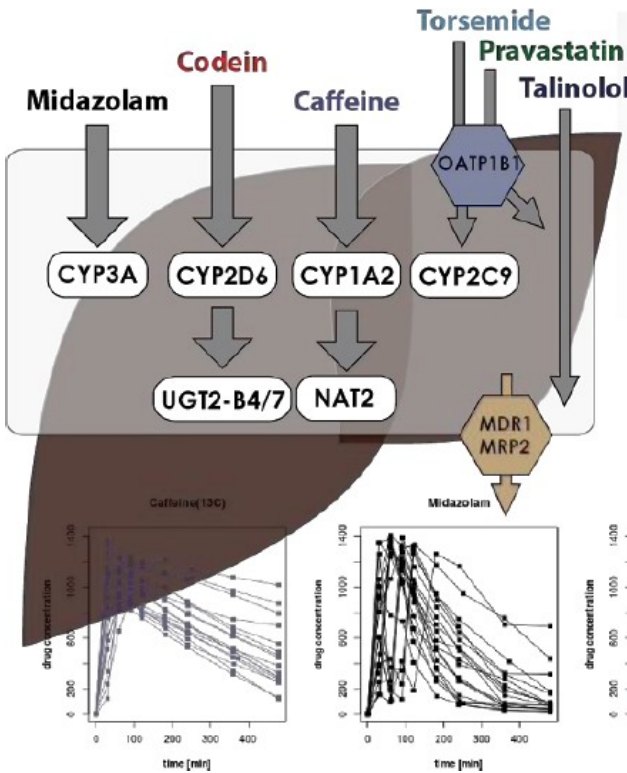
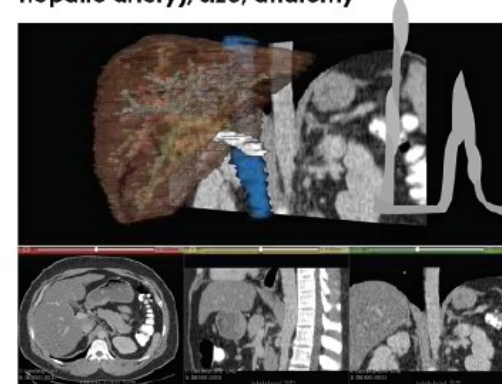


Figure 1 - Overview of the five work packages and their interconnection with description provided in the main text. The standardization of all data and workflows is crucial for the individual work packages. All data will be managed via central standardized data management.



Liver blood flow (portal vein & hepatic artery), size, anatomy



Lifestyle questions
anthropomorphic information



Spiroergometry
Physical fitness



Study	Number of kinetics	MRT	Spirometry	PK data	4β-OH-Cholest. Total cholesterol	Urine caffeine-metabolite & 6β-OH-Cortisol/Cortisol
IKP 243	103	60	59	103	103	ongoing
IKP 243 2nd day	18	-	18	18	18	ongoing
2 planned	-	-	-			
IKP260 twins	74 (37 twin pairs)	34	32	74	74	ongoing

Table 2 - Overview clinical studies of drug cocktails at IKP (status 02-2015).

Number of patients	Number of kinetics	PK data	4β-OH-Cholest. Total cholesterol	Urine caffeine-metabolite & 6β-OH-Cortisol/Cortisol
82	81	81	81	ongoing
additionally planned: 18				

Table 3 - Overview clinical study project G1 (patient study in Kiel), status 13-02-2015.

Bioinformatics software

König M. and Holzhütter HG.

FluxViz - Cytoscape Plug-in for Vizualisation of Flux Distributions in Networks
Genome Informatics 2010, Vol.24, p.96-103

König M., Dräger A. and Holzhütter HG.

CySBML: a Cytoscape plugin for SBML
Bioinformatics. 2012 Jul 5.

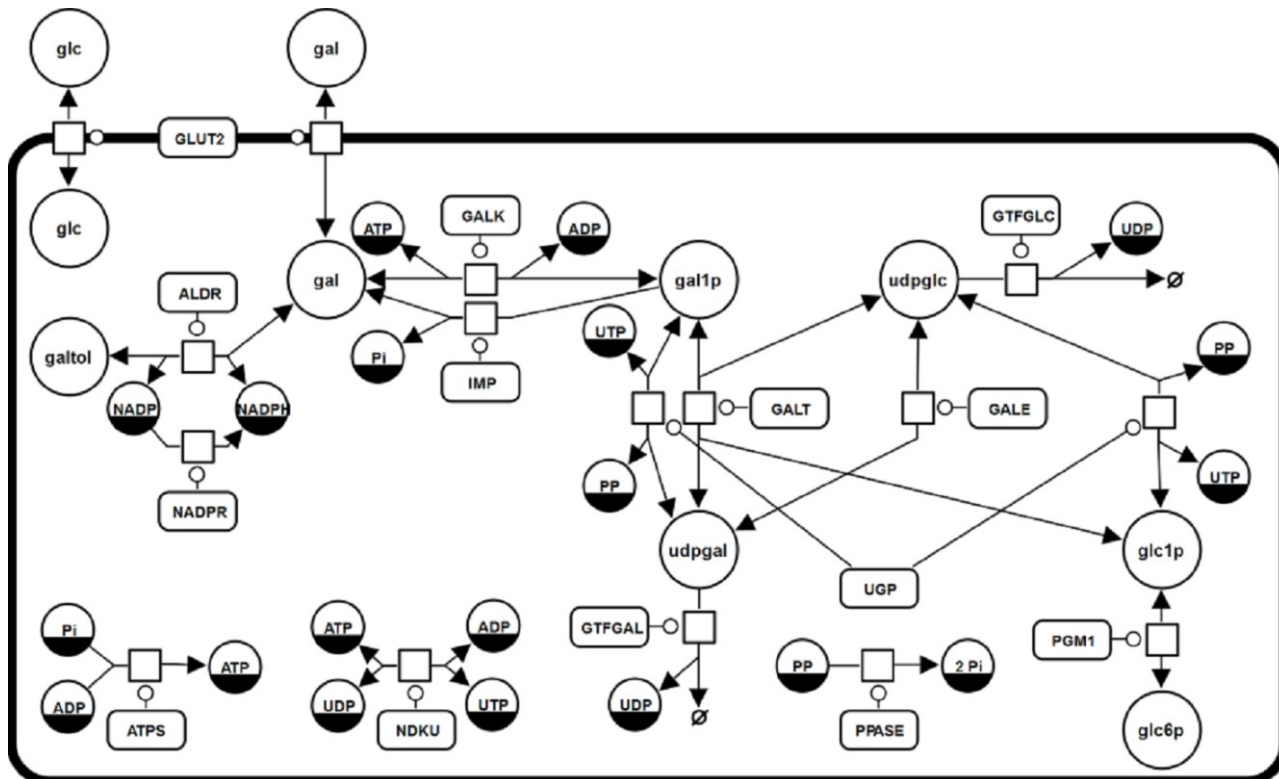
Somogyi ET., Bouteiller JM., Glazier JA., **König M.**, Medley JK., Swat MH and Sauro HM.

LibRoadRunner: a high performance SBML simulation and analysis library.

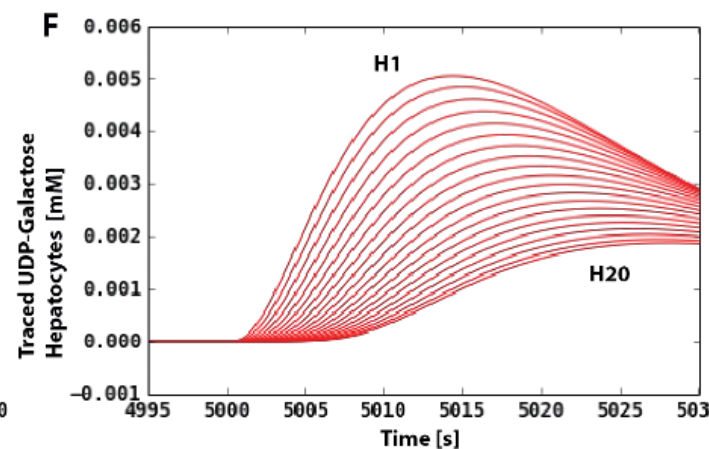
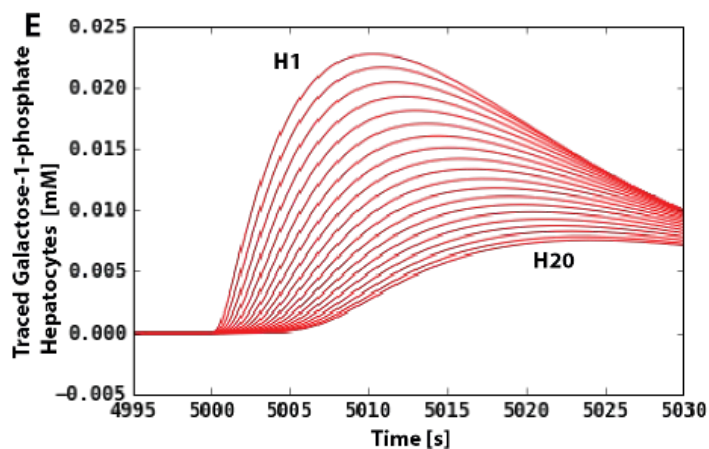
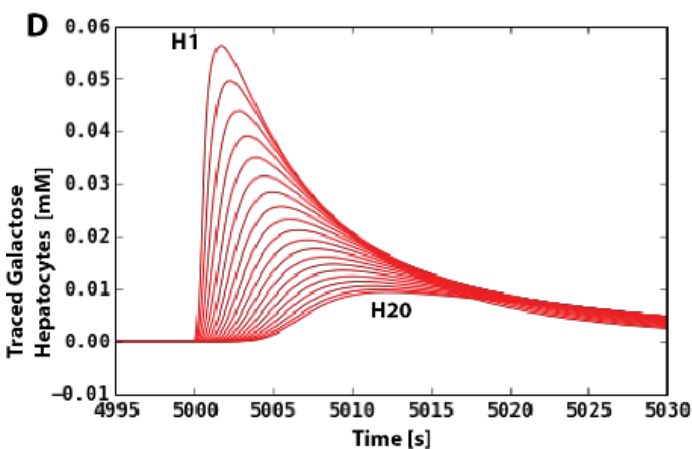
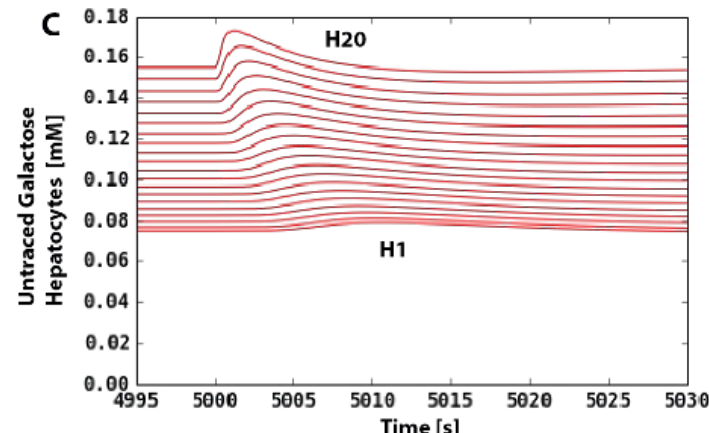
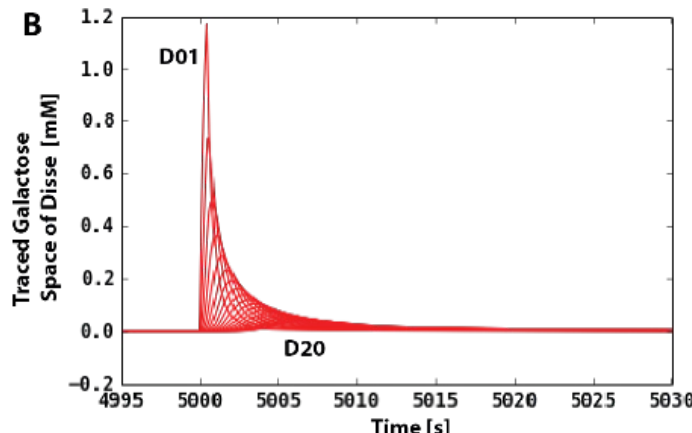
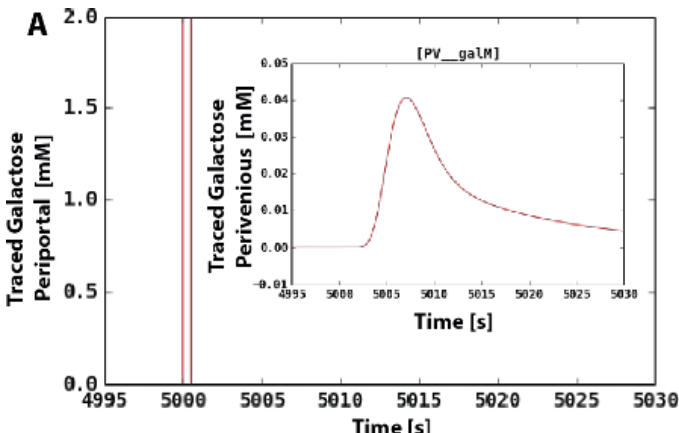
Bioinformatics. 2015 Jun 17. pii: btv363.

GALACTOSE METABOLISM

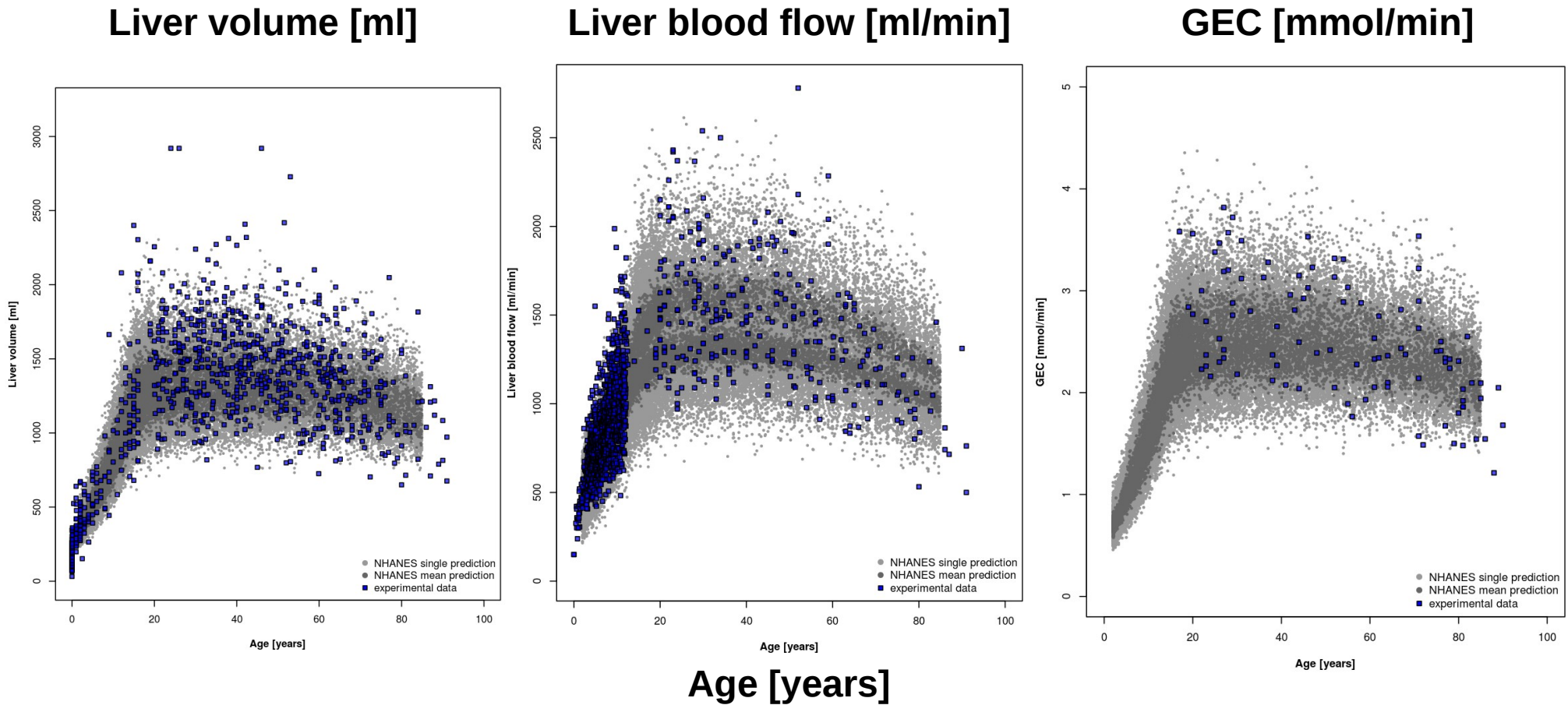
- Kinetic ODE model for single cells
- Main enzymatic steps
 - I. **Galactokinase (GALK)**
phosphorylation of galactose (gal) to galactose 1-phosphate (gal1p) catalysed
 - II. **Galactose-1-phosphate uridyl transferase (GALT)**
conversion of gal1p to UDP-galactose (udpgal)
 - III. **UDP-galactose 4'-epimerase (GALE)**
interconversion of udpgal and UDP-glucose (udpglc)



Sinusoidal gradients



Predicted liver volumes, blood flow & GEC



Predictions (grey) uses anthropomorphic dataset from NHANES cohort ($N>10000$). Statistical models (GAMLSS) based on anthropomorphic trainings sets.

http://www.cdc.gov/nchs/nhanes/about_nhanes.htm

Experimental data (blue) from multiple studies measuring liver volumes & blood flow

All data points are single individuals.

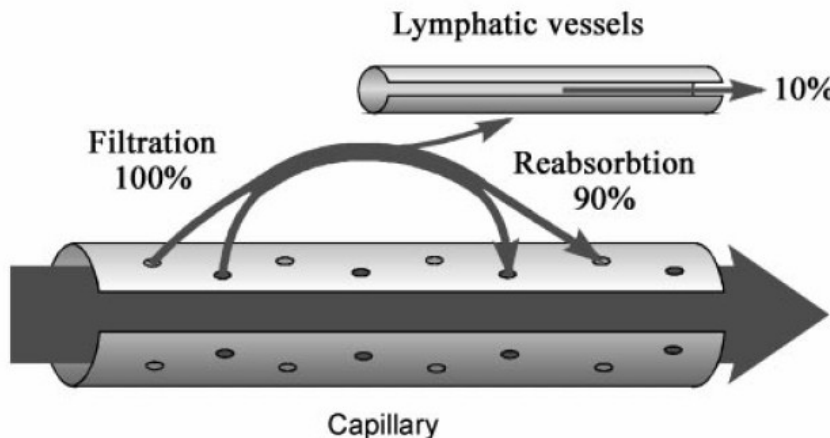


FIG. 1.

A: scheme of pressure distribution along capillary and flow exchange between capillary and tissue in muscle. P , pressure; P_{hc} , hydrostatic pressure of blood in capillary; P_{ht} , tissue hydrostatic pressure; P_a , pressure at arterial end of capillary; P_b , pressure at venous end of capillary; P_0 , oncotic pressure; P_{oc} , oncotic pressure of plasma; P_{ot} , oncotic pressure of tissue fluid; L , length of capillary. B: scheme of blood-tissue fluid exchange in blood capillary and lymphatics.

- Model of pressure and flow dependency in the sinusoidal unit based on analytical solutions for filtration and reabsorption in capillaries depending on ultrastructural parameter
 - **W**: specific hydraulic resistance of the capillary with R radius of sinusoid
 - **ω** : hydraulic resistance of all pores (fenestrae) at capillary surface with r radius of pore, I capillary thickness, n pore density
 - **$P(x)$** : pressure along sinusoid
 - **$Q(x)$** : flow along sinusoid
 - **$q(x)$** : pore flow

Pressure dependent Fluid transport

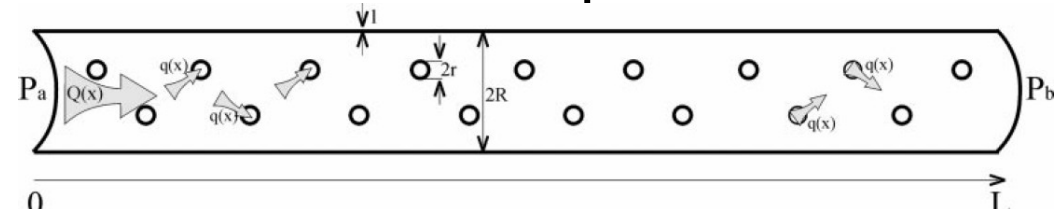


FIG. 2.

Model of capillary with pores in its wall. P_a and P_b are pressures at arterial ($x = 0$) and venous ($x = L$) ends of capillary, where x represents distance along length of capillary. $2R$, diameter of capillary; $2r$, diameter of pore; $Q(x)$, flow along capillary; $q(x)$, flow through pores.

$$W = \frac{8\eta}{\pi R^4} \quad \omega = \frac{4\eta I}{\pi^2 I^4 R n} \quad \lambda = \sqrt{\frac{\omega}{W}} = \sqrt{\frac{R^3 I}{2\pi I^4 n}}$$

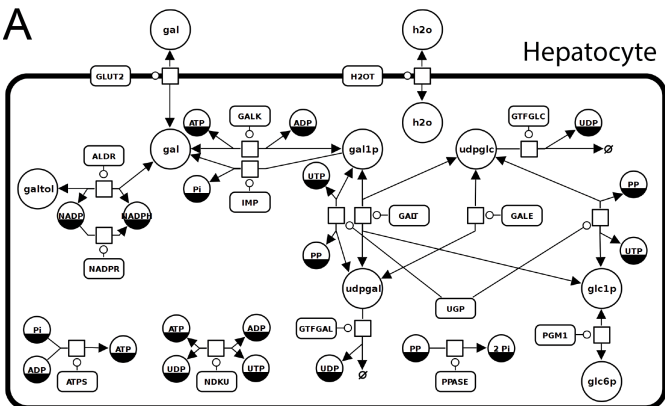
$$P(x) = \frac{-(P_b - P_0) + (P_a - P_0)e^{-L/\lambda}}{e^{-L/\lambda} - e^{L/\lambda}} e^{x/\lambda} + \frac{(P_b - P_0) - (P_a - P_0)e^{L/\lambda}}{e^{-L/\lambda} - e^{L/\lambda}} e^{-x/\lambda} + P_0$$

$$Q(x) = -\frac{1}{\sqrt{W\omega}} \left[\frac{-(P_b - P_0) + (P_a - P_0)e^{-L/\lambda}}{e^{-L/\lambda} - e^{L/\lambda}} e^{x/\lambda} - \frac{(P_b - P_0) - (P_a - P_0)e^{L/\lambda}}{e^{-L/\lambda} - e^{L/\lambda}} e^{-x/\lambda} \right]$$

$$q(x) = \frac{1}{\omega} \left[\frac{-(P_b - P_0) + (P_a - P_0)e^{-L/\lambda}}{e^{-L/\lambda} - e^{L/\lambda}} e^{x/\lambda} + \frac{(P_b - P_0) - (P_a - P_0)e^{L/\lambda}}{e^{-L/\lambda} - e^{L/\lambda}} e^{-x/\lambda} \right]$$

Transport & Metabolism

- Diffusion & convection are modeled via discretized one-dimensional equations based on local flow $Q(x)$, $q(x)$ and concentrations $c(x)$
- Diffusion through sinusoidal fenestrae is described via pore theory (sterical hindrance depending on molecule sizes)
- Metabolic models (ODE) based on detailed kinetic equations for the enzymes in galactose pathway in all hepatocyte along the sinusoid



Convection

$$V_{Si \rightarrow Sj}^{conv}(k) = Q_{Si} \cdot c_{Si}(k)$$

Filtration & reabsorption

$$V_{Si \rightarrow Di}^{conv}(k) = q_{Si} \cdot \Delta x \cdot c_{Si}(k)$$

Diffusion in sinusoid

$$V_{Si \rightarrow Sj}^{diff}(k) = \frac{D_{k,0}}{\Delta x \cdot A_{sin}} \cdot (c_{Si}(k) - c_{Sj}(k))$$

Diffusion sinusoid & space of Disse

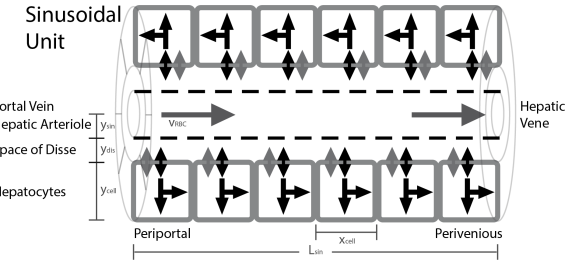
$$V_{Si \rightarrow Di}^{diff}(k) = \frac{D_{k,a}}{\Delta y \cdot A_{sin-disse} \cdot f_{fen}} \cdot (c_{Si}(k) - c_{Di}(k))$$

$$\frac{D_a}{D_{a,0}} = \left(1 - \frac{r_a}{r_{fen}}\right)^2 \left[1 - 2.104\left(\frac{r_a}{r_{fen}}\right) + 2.09\left(\frac{r_a}{r_{fen}}\right)^3 - 0.95\left(\frac{r_a}{r_{fen}}\right)^5 \right]_{her1953}$$

Diffusion space of Disse

$$V_{Di \rightarrow Dj}^{diff}(k) = \frac{D_{k,0}}{\Delta x \cdot A_{disse}} \cdot (c_{Di}(k) - c_{Dj}(k))$$

Reactions [72]	name	reversibility	equation	modifiers	derived units	formula
C01_ATPS	ATP synthase [C01_]	<=>	C01_adp + C01_phos <=> C01_atp	mole * s^-1		C01_ATPS_Vmax / (ATPS_k_adp * ATPS_k_phos) * (C01_adp * C01_phos - C01_atp / ATPS_k_cat) / ((1 + C01_adp / ATPS_k_adp) * (1 + C01_phos / ATPS_k_phos) + C01_atp / ATPS_k_cat)
C01_ALDR	Aldose reductase [C01_]	<=>	C01_gal + C01_nadph <=> C01_galM C01_galtol + C01_nadp	C01_galM mole * s^-1		C01_gal / C01_gal_tot * C01_ALDR_Vf - C01_galtol / C01_galtol_tot * C01_ALDR_Vb
C01_GALK	Galactokinase [C01_]	<=>	C01_gal + C01_atp <=> C01_gal1p + C01_adp	C01_galM mole * s^-1		C01_gal / C01_gal_tot * C01_GALK_Vf - C01_gal1p / C01_gal1p_tot * C01_GALK_Vb
C01_IMP	Inositol monophosphatase [C01_]	=>	C01_gal1p => C01_gal + C01_phos	C01_gal1pM mole * s^-1		C01_gal1p / C01_gal1p_tot * C01_IMP_Vf



Perfusion CT

Table 1
Estimated perfusion values of the liver of normal and disease groups.

	HAP (ml/min/100 ml)	HPP (ml/min/100 ml)	APF (%)
Normal group (<i>n</i> = 30)			
Subsegment			
1	30.3 ± 10.1	131.4 ± 61.1	21.5 ± 10.2
2	28.5 ± 10.3	107.3 ± 45.5	25.0 ± 10.8
3	29.3 ± 11.4	95.6 ± 36.5	26.4 ± 9.2 ^a
4	25.0 ± 11.2	116.3 ± 53.2	21.0 ± 10.5
5	23.3 ± 8.5	118.7 ± 39.3	18.6 ± 8.0 ^a
6	24.1 ± 8.5 ^b	116.7 ± 40.1	19.3 ± 7.3 ^c
7	23.2 ± 7.4	114.0 ± 42.7	19.5 ± 7.4
8	24.0 ± 8.5	118.3 ± 42.3	19.6 ± 8.9
Disease group (<i>n</i> = 8)	31.0 ± 5.9 ^b	80.7 ± 39.2	37.2 ± 19.0 ^c

APF, arterial perfusion fraction; HAP, hepatic arterial blood flow; HPP, hepatic portal perfusion.

^a Mean APF of subsegment 3 was significantly higher than that of subsegment 5 (*p* < 0.01).

^b Mean HAP in the disease group was significantly higher than that in the normal group (*p* < 0.05).

^c Mean APF in the disease group was significantly higher than that in the normal group (*p* < 0.0005).

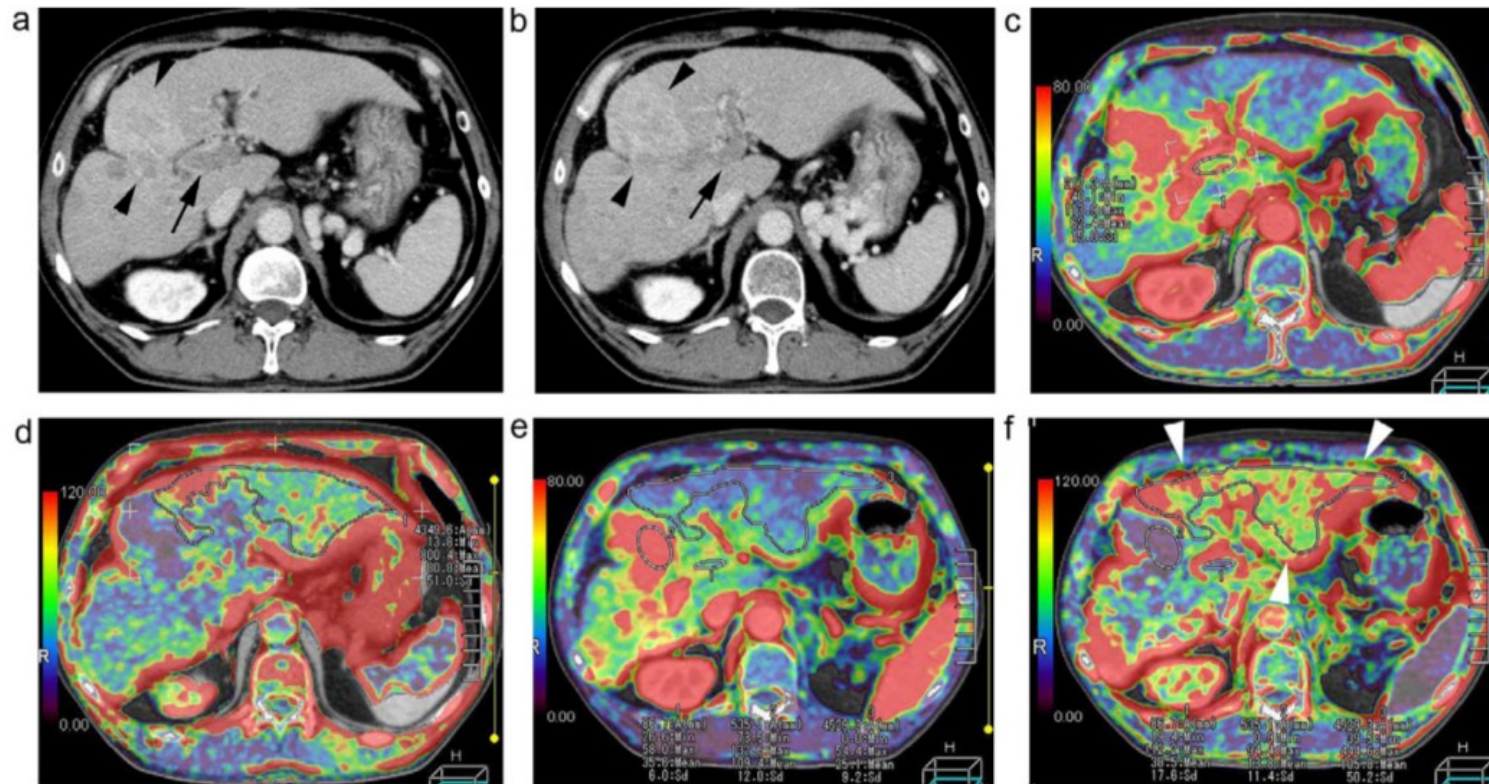
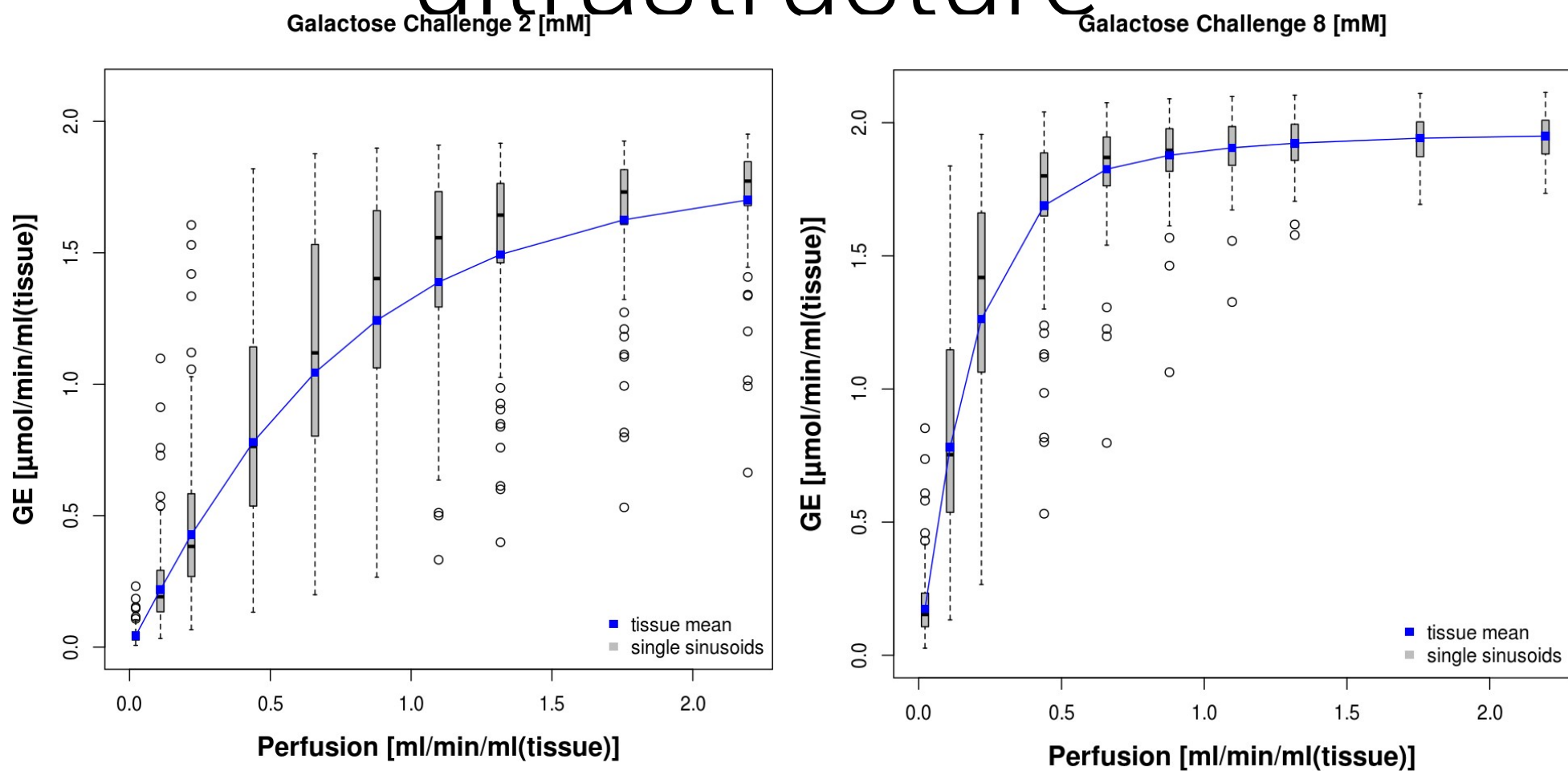


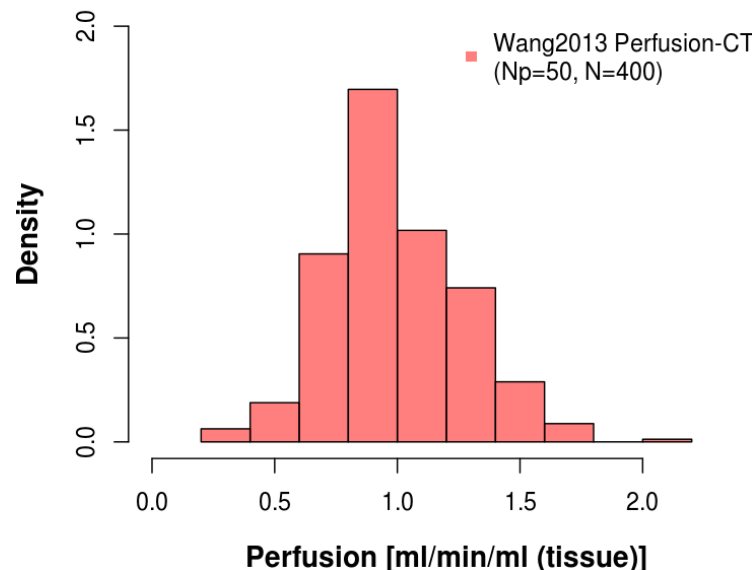
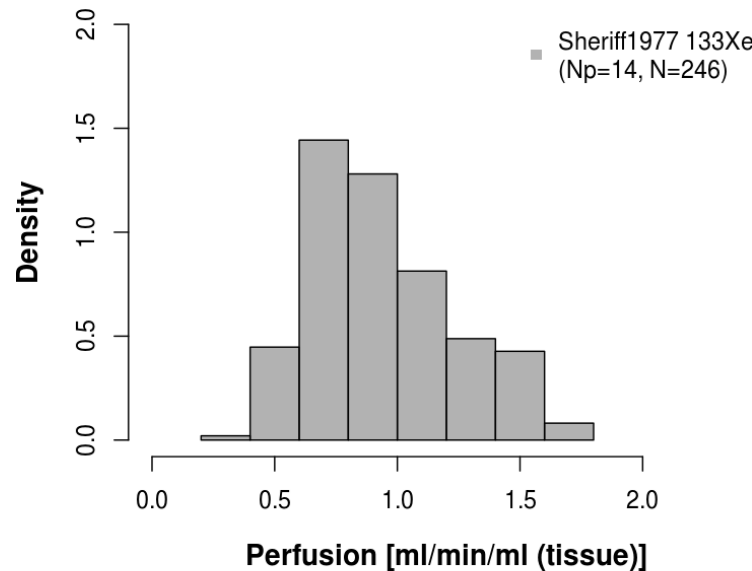
Fig. 2. A 60-year-old man with clinically diagnosed hepatocellular carcinoma accompanied by intra-portal tumor invasion. Contrast-enhanced CT images at time of the first CT perfusion are shown as (a) and (b). He received transcatheter chemoembolization for intra-hepatic tumors ((a) and (b), arrowheads) and radiation therapy for intra-portal tumor invasion ((a) and (b), arrows). CT hepatic arterial perfusion map (c) shows an increase in arterial perfusion in the intra-portal tumor and the portal perfusion map (d) shows a decrease in portal perfusion in the non-cancerous parenchyma. Following CT perfusion 1 week after the end of radiation therapy, the hepatic arterial perfusion map (e) shows a decrease in arterial perfusion in the intra-portal tumor and the portal perfusion map (f) shows recovery of portal perfusion, especially in left lobe of the liver (arrowheads).

Heterogeneity in galactose elimination due to ultrastructure

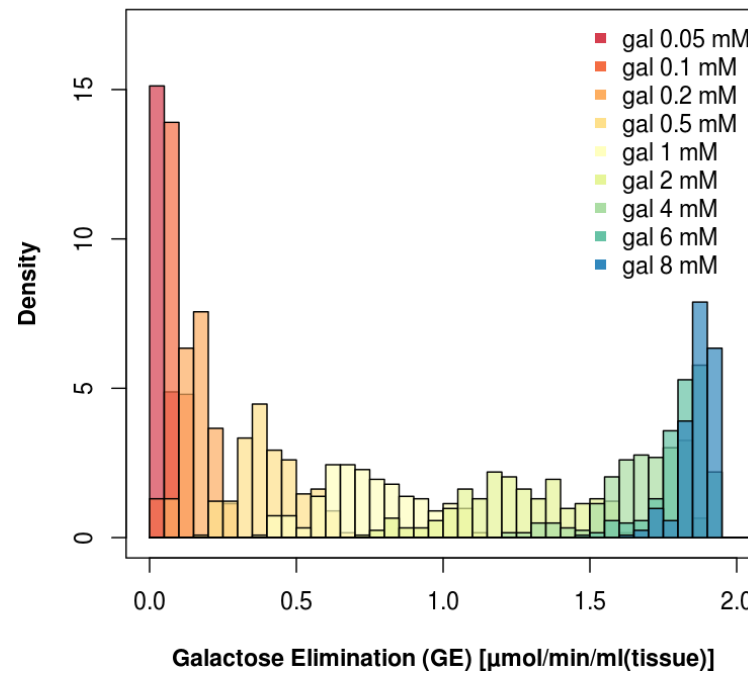


Perfusion Heterogeneity

Perfusion Heterogeneity (CT & Xe)



Galactose Elimination Sheriff1977 (age=20)



- Distribution of perfusion heterogeneity in liver similar with 133Xe & CT measurements
- The local distribution of perfusion results in distributions of galactose elimination
- Width and shape of perfusion distribution is transformed depending on actual galactose concentration
- Analog the GE can be calculated locally in perfusion-CT